Discovery and characterization of a sulfoquinovose mutarotase using kinetic analysis at equilibrium by exchange spectroscopy

Palika Abayakoon,[1,2] James P. Lingford,[3,4] Yi Jin,[5] Christopher Bengt,[1,2] Gideon J. Davies,[5] Shenggen Yao,[2]* Ethan D. Goddard-Borger,[3,4]* Spencer J. Williams[1,2]*

1 School of Chemistry, University of Melbourne, Parkville, Vic 3010 (Australia)

2 Bio21 Molecular Science and Biotechnology Institute, University of Melbourne, Parkville, Vic 3010 (Australia)

3 ACRF Chemical Biology Division, The Walter and Eliza Hall Institute of Medical Research, Parkville, Vic 3052 (Australia)

4 Department of Medical Biology, University of Melbourne, Parkville, Vic 3010 (Australia)

5 York Structural Biology Laboratory, Department of Chemistry, University of York, Heslington, YO10 5DD (UK)

Abstract

Bacterial sulfoglycolytic pathways catabolise sulfoquinovose (SQ), or glycosides thereof, to generate a three-carbon metabolite for primary cellular metabolism and a three-carbon sulfonate that is expelled from the cell. Sulfoglycolytic operons encoding an Embden-Meyerhof-Parnas (EMP)-like or Entner-Doudoroff (ED)-like pathway harbour an uncharacterized gene (*yihR* in *Escherichia coli*; *PpSQ1_00415* in *Pseudomonas putida*) that is upregulated in the presence of SQ and has been annotated as an aldose-1-epimerase and which may encode an SQ mutarotase. Our sequence analyses and structural modelling confirmed that these proteins possess mutarotase-like active sites with conserved catalytic residues. We over-expressed the homologue from the sulfo-ED operon of *Herbaspirillum seropedicaea* (*Hs*SQM) and used it to demonstrate SQ mutarotase activity for the first time. This was accomplished using NMR exchange spectroscopy (EXSY), a method that allows chemical exchange of magnetization between the two SQ anomers at equilibrium. *Hs*SQM also catalyzed the mutarotation of various aldohexoses with an equatorial 2-hydroxy group, including D-galactose, D-glucose, D-glucose-6-phosphate, and D-glucuronic acid, but not D-mannose. *Hs*SQM displayed only 5-fold selectivity in terms of efficiency (k_{cat}/K_M) for SQ versus the glycolysis intermediate glucose-6-phosphate (Glc-6-P), however its proficiency [k_{uncat} / (k_{cat}/K_M)] for SQ was 17,000-fold better than for Glc-6-P, revealing that *Hs*SQM preferentially stabilises the SQ transition state.

Introduction

Various prokaryotes metabolise the sugar sulfoquinovose (SQ) to sulfolactaldehyde (SLA) and dihydroxyacetone phosphate (DHAP), via an Embden-Meyerhof-Parnas (EMP)-like pathway [1], or pyruvate, via an Entner-Doudoroff (ED)-like pathway [2, 3] (Figure 1). While the DHAP or pyruvate feed into primary metabolic pathways, SLA is converted to 2,3-dihydroxypropanesulfonate (DHPS) or sulfolactate (SL) by the sulfo-EMP and sulfo-ED pathways, respectively, and excreted from the cell. Yet sulfoquinovose is rarely encountered as a free sugar in nature; rather it is liberated from the plant sulfolipid α-sulfoquinovosyl diacylglycerol (SQDG), or its delipidated form α-sulfoquinovosyl glycerol (SQGro), by the action of glycoside hydrolases termed sulfoquinovosidases (SQases) [4]. SQases are retaining glycosidases, and result in the initial formation of α-SQ, which can undergo mutarotation to β-SQ at an unknown rate. The anomeric preferences of the immediate downstream enzymes that utilize SQ (SQ isomerase for the sulfo-EMP pathway; SQ dehydrogenase for the sulfo-ED pathway) are unknown.

All proteins comprising a sulfo-ED or sulfo-EMP pathway are typically encoded within a single gene cluster. These clusters usually include an SQase, which highlights that SQ glycosides are important natural feedstocks for sulfoglycolytic pathways [1, 2]. The gene clusters also encode a conserved uncharacterized protein, annotated as an aldose-1-epimerase, which likely catalyses SQ mutarotation: an enzyme activity yet to be reported. Mutarotases are widely distributed enzymes that facilitate the rapid mutarotation of aldoses to enhance flux through metabolic pathways when enzymes acting on reducing sugars are specific for a single anomer [5, 6].

A classical approach to studying mutarotases involves measuring rates of mutarotation by polarimetry [7-10]. These assays are limited by an inability to prepare pure samples of a single anomer of many reducing sugars. Indeed, to date it has not been possible to obtain SQ as a single anomer, which makes this approach of limited use for studying putative SQ mutarotases (SQMs). Alternative approaches to studying mutarotases have employ coupled assays in which only one anomer acts as substrate for a secondary enzyme [11, 12] or a chemical reaction (e.g. bromine oxidation [13]), or use a glycosidase to prepare a single anomer in solution prior to addition of the mutarotase [12]. The high rate of uncatalyzed mutarotation under standard conditions often renders these assays technically demanding, and a requirement for different coupling enzymes for each substrate undermines their generality. An alternative approach is to study reaction rates at equilibrium. NMR spectroscopy is ideally suited to this

approach using the technique of exchange spectroscopy (EXSY) [14, 15]. EXSY involves chemical shift labelling of the spin population of nuclei at one site within a substrate, followed by a chemical reaction that changes the chemical environment of individual nuclei resulting in magnetization transfer to the new site, and finally sampling of the magnetization states of the nuclei in the substrate and product. Because of the spectral resolution of NMR spectroscopy and the potential to conduct two-dimensional variants, EXSY can be used to study unidirectional reactions at equilibrium. Several reports have described the development of saturation transfer and inversion transfer NMR methods for analysis of equilibrium exchange rates for mutarotases [16-19].

Here, we disclose the first measurement of SQ mutarotase activity, using an enzyme from *Herbaspirillum seropedicaea* (*Hs*SQM) and 2D EXSY, and analyze its selectivity for various reducing sugars with and without an anionic substituent at C6. *Hs*SQM exhibited a broad spectrum of activity for sugars with an equatorial hydroxyl group at C2 and with, or without, charge at C6. 1D EXSY was used to measure reaction rates to obtain Michaelis-Menten kinetics for *Hs*SQM with SQ and glucose-6-phosphate, a common cytoplasmic metabolite, revealing an approximate 5-fold preference for SQ as a substrate. Sequence and structural analyses revealed *Hs*SQM belongs to the galactose mutarotase-like Structural Classification Of Proteins (SCOP) with strictly conserved active site residues that are proposed to be involved in substrate binding and catalysis.

Materials and Methods

Reagents

D-Glucose (Glc), D-mannose (Man), D-galactose (Gal), D-glucuronic acid (GlcA) and D-glucose-6-phosphate (Glc-6-P) were purchased from Sigma Aldrich. D-Sulfoquinovose was purchased from MCAT GmbH (Germany, http://www.MCAT.de). 4-Nitrophenyl α-D-sulfoquinovoside and sulfoquinovosidase have been described previously [4].

Cloning, expression and purification of HsSQM

A gene encoding the *Herbaspirillum seropedicaea* strain AU14040 protein WP_069374721.1 was codon harmonised for *E. coli*, synthesised and cloned into the pET29 vector using the *NdeI* and *XhoI* restriction sites to provide pET29-HsSQM (see Supporting Information). This plasmid was transformed into chemically competent 'NEB Express' *E. coli*, plated onto LB-agar (50 µg/ml kanamycin) and incubated at 37 °C for 16 h. A single colony was used to inoculate 10 ml of LB media containing 50 µg/ml kanamycin followed by incubation at 37 °C for 16 h. This culture was used to inoculate 1000 ml of "S-broth" (35 g tryptone, 20 g yeast extract, 5 g NaCl, pH 7.4) containing 50 µg/ml kanamycin, which was incubated with shaking (250 rpm) at 37°C until it reached an OD_{600} of 0.7. The culture was cooled to room temperature, IPTG added to a final concentration of 100 µM, and then incubated with shaking (200 rpm) at 18 °C for 19 h. The cells were harvested by centrifugation at 17,000 *g* for 20 min at 4 °C then resuspended in 40 ml of binding buffer (50 mM NaP_i, 500 mM NaCl, 5 mM imidazole, pH 7.5) containing protease inhibitor (Roche complete EDTA-free protease inhibitor cocktail) and lysozyme (0.1 mg/ml) by nutating at 4 °C for 30 min. Benzonase (1 µl) was added to the mixture and lysis was effected by sonication. The lysate clarified by centrifugation (17,000 *g* for 20 min at 4 °C), the supernatant filtered (0.45 µm) and loaded onto a 1 ml HiTrap TALON column (GE Healthcare). The column was washed with 15 ml binding buffer and the protein was eluted using elution buffer (50 mM NaP_i, 500 mM NaCl, 500 mM imidazole, pH 7.5). Fractions containing the protein of interest (as determined by SDS-PAGE) were further purified by size exclusion chromatography on a HiLoad 16/600 Superdex 75 column using 50 mM NaP_i, 150 mM NaCl, pH 7.5. Fractions containing the protein of interest were further purified on a MonoQ 5/50 column with protein bound in buffer A (20 mM Tris, pH 7.5) and eluted with a linear gradient from 100% buffer A to 100% buffer B (20 mM Tris, NaCl 500 mM, pH 7.5) over 15 ml at 1 ml/min. Protein yield was ≈5 mg per litre of culture.

NMR magnetization-transfer experiments

The theoretical background of NMR for the study of kinetics of chemical exchange has been well documented [14, 20] and only a brief overview is presented. The interconversion of anomers by mutarotation is described by a simple two-state equilibrium:

$$\alpha \underset{k_{-1}}{\overset{k_1}{\rightleftharpoons}} \beta \tag{1}$$

For a species exchanging between isomers, the dependence upon time (t) of the longitudinal nuclear magnetizations of corresponding nuclei from the α and β anomer spin populations (I_α) and (I_β), corresponding to the integrals, are given by the Bloch-McConnell equation:

$$\frac{d}{dt}\begin{pmatrix} I_\alpha \\ I_\beta \end{pmatrix} = \begin{pmatrix} -R_\alpha - k_1 & k_{-1} \\ k_1 & -R_\beta - k_{-1} \end{pmatrix}\begin{pmatrix} I_\alpha \\ I_\beta \end{pmatrix} + \begin{pmatrix} R_\alpha & 0 \\ 0 & R_\beta \end{pmatrix}\begin{pmatrix} I_\alpha^0(t) \\ I_\beta^0(t) \end{pmatrix} \tag{2}$$

Where R_α and R_β are the longitudinal relaxation rates, characterizing the return of the magnetizations towards their respective equilibrium values, I_α^0 and I_β^0; k_1 and k_{-1} are the extrinsic rate constants for the forward and reverse reactions for each anomer, α and β respectively. The solution of this equation gives the intensity of the transferred magnetization at τ_{mix}:

$$\begin{pmatrix} I_\alpha(\tau_{\mathrm{mix}}) \\ I_\beta(\tau_{\mathrm{mix}}) \end{pmatrix} = \exp\left[\begin{pmatrix} -R_\alpha - k_1 & k_{-1} \\ k_1 & -R_\beta - k_{-1} \end{pmatrix}\tau_{\mathrm{mix}}\right] \times \begin{pmatrix} I_\alpha(0) - I_\alpha^0 \\ I_\beta(0) - I_\beta^0 \end{pmatrix} + \begin{pmatrix} I_\alpha^0 \\ I_\beta^0 \end{pmatrix} \tag{3}$$

Under the condition of chemical equilibrium, the net flux is zero. However, the unidirectional fluxes remain and are equal in both directions. Thus,

$$k_1[\alpha]^{\mathrm{eq}} = k_{-1}[\beta]^{\mathrm{eq}} \tag{4}$$

And

$$K_{\mathrm{eq}} = \frac{[\beta]^{eq}}{[\alpha]^{\mathrm{eq}}} = \frac{k_1}{k_{-1}} = \exp\left(-\frac{\Delta G}{RT}\right) \tag{5}$$

To obtain the rate constants, k_1 and k_{-1}, at a given concentration ratio of the substrate and enzyme, a series of 1D ^{1}H EXSY spectra with mixing time τ_{mix}, ranging from 5 ms to 1.5 s were acquired using a 1D selective NOESY pulse sequence. For each substrate concentration, the normalized integrals of the substrate (H1α) and product (H1β) anomeric signals are plotted against mixing time, providing buildup and decay curves, respectively, as described previously [21]. The data were then fitted to a second-order polynomial, an approximation to Eq 3, which is valid for short mixing times. The tangent at $\tau_{\mathrm{mix}} = 0$, the so-called initial rate approach [22], provides estimates of both exchange-rate constants k_1 and k_{-1}.

Michaelis–Menten kinetics

The equilibrium-exchange kinetics (reaction rate, v^{eq}) of a mutarotase-mediated reaction can be expressed as:

$$v^{\mathrm{eq}}([\alpha]) = \frac{V_{\mathrm{max}}^{\mathrm{eq}}[\alpha]}{K_{\mathrm{M}}^{\mathrm{eq}} + [\alpha]} \tag{9}$$

$V_{\mathrm{max}}^{\mathrm{eq}}$ is the maximum rate of reaction, reached under saturating equilibrium exchange conditions when [α] >> $K_{\mathrm{M}}^{\mathrm{eq}}$. The rate of the mutarotation process can be expressed in terms of the Michaelis-Menten equation:

$$v^{eq} = k_1[\alpha]^{\mathrm{eq}} = \frac{V_{\mathrm{max}}^{\mathrm{eq}}[\alpha]}{K_{\mathrm{M}}^{\mathrm{eq}} + [\alpha]} \tag{10}$$

k_{cat} is calculated by dividing $V_{\mathrm{max}}^{\mathrm{eq}}$ by the enzyme concentration.

2D ^{1}H-^{1}H EXSY experiments

2D ^{1}H-^{1}H EXSY spectra for all substrates (SQ, Glc-6-P, Glc, Gal, Man, GlcA) were acquired at 25 ºC on a Bruker Avance II 800 spectrometer equipped with a TXI cryoprobe using the standard 2D NOESY/EXSY pulse sequence (noesyphpr). Spectra were collected with 4 and 8 scans in the absence and presence of enzyme, respectively. A mixing time, τ_{mix} of 1.1 s was used for all the experiments. Spectra were processed and analysed using TOPSPIN (version 3.2 Bruker) and ^{1}H chemical shifts were referenced indirectly to DSS at 0 ppm via the H_2O resonance, 4.77 ppm at 25 ºC. Samples were prepared in D_2O buffer consisting of 50 mM

182 sodium phosphate, 150 mM NaCl (pD 7.5) with a substrate concentration 5 mM in the absence
183 or presence of 1.51 μM *Hs*SQM. pD was measured using a pH meter and the relationship pD
184 = pH + 0.4.
185
186 **1D ^{1}H EXSY experiments**
187 *Michaelis-Menten parameters*
188 1D ^{1}H EXSY spectroscopic studies for SQ and Glc-6-P were performed at 25 °C on a Bruker
189 Avance III 600 spectrometer equipped with a TCI cryoprobe using a 1D selective NOESY
190 pulse sequence (selnogp, Bruker). Samples were prepared in D_2O buffer consisting of 50 mM
191 sodium phosphate, 150 mM NaCl (pD 7.5) using 1.50 μM *Hs*SQM at substrate concentrations
192 ranging from 0.5-15.0 mM (for SQ) or 0.5-30.0 mM (for Glc-6-P). pD values were calculated
193 using the following relationship: pD = pH + 0.4. For each sample, 1D ^{1}H EXSY spectra with
194 mixing time, τ_{mix}, ranging from 5 ms to 1.5 s were acquired with number of scans varying
195 between 32 and 256 depending on the concentration of substrate. A recycle delay of 13.4 s (c.a.
196 3-5 times of measured ^{1}H T_1 relaxation times) between scans was used for the acquisition of
197 1D ^{1}H EXSY spectra. Spectra were subsequently processed and analysed using TOPSPIN
198 (version 3.2 Bruker). Kinetic data for conversion of the β-anomer of SQ to the α-anomer were
199 obtained by selectively inverting the resonance of H5β at 3.72 ppm using a Gaussian-shaped
200 pulse of 20 ms, and *vice versa*, for conversion of the α-anomer to the β-anomer, the same
201 selective pulse was applied to the resonance of H5α at 4.15 ppm. Similarly, for the conversion
202 of the β-anomer of Glc-6-P to the α-anomer, kinetic data were obtained by selectively inverting
203 the signal for H1β at 4.57 ppm. A build-up curve for the β-anomer could not be obtained since
204 the signal for H1β at 4.57 ppm was affected by the nearby HOD peak at 4.77 ppm (see SI data
205 for representative ^{1}H NMR spectra). Instead, the rate constant for the conversion of the α-
206 anomer to the β-anomer were calculated using Eq 4. Rates for each concentration were
207 calculated using the Prism 6 software package (GraphPad Scientific Software). Data were fitted
208 to a second-order polynomial function as described previously by Aski *et al*. [21].
209
210 *pD dependence of activity for* Hs*SQM*
211 The Michaelis-Menten parameter k_{cat}/K_M was measured for Glc-6-P mutarotation in D_2O buffer
212 consisting of 50 mM citrate/phosphate, 150 mM NaCl at a range of pD values (5.6, 6.1, 6.5,
213 7.0, 7.5, 8.1, 9.0, 9.4, 9.8, 10.4 and 10.9) at 25 ºC. Reactions were initiated by adding 1.48-
214 2.96 μM *Hs*SQM to Glc-6-P (5.0 mM) in buffer and the rate measured by 1D ^{1}H EXSY as

215 described above with mixing time, τ_{mix}, ranging from 5 ms to 1.0 s and number of scans from
216 64 and 128. Kinetic data were obtained for the conversion of the β-anomer of Glc-6-P to the α-
217 anomer, by selectively inverting the signal for H1β at 4.57 ppm. k_{cat}/K_M and pK_a values were
218 calculated using the Prism 6 software package (Graphpad Scientific Software). pH dependence
219 was fit to the following function:

220 $$y = \frac{k_{\mathrm{cat}}}{K_{\mathrm{M}}}\left[\left(\frac{1}{1+\left(\frac{10^{-\mathrm{pH}}}{10^{-\mathrm{p}Ka1}}+\frac{10^{-\mathrm{p}Ka2}}{10^{-\mathrm{pH}}}\right)}\right)\right] + c \quad (11)$$

221

222 **Uncatalyzed mutarotation rate measurement**

223 The uncatalyzed rate constant for SQ mutarotation was measured using polarimetry on a Jasco
224 DIP-1000 digital polarimeter equipped with Na 589 nm lamp and 100.00 mm cell, using a
225 sulfoquinovosidase to generate α-SQ from 4-nitrophenyl α-D-sulfoquinovoside (PNPSQ).
226 Analysis by ^{1}H NMR spectroscopy and thin layer chromatography revealed that hydrolysis of
227 PNPSQ was complete within 5 min. SQase (final concentration 2.13 μM) was added to a
228 solution of PNPSQ (final concentration 12.4 mM) in buffer in a final volume of 2 ml. Buffers
229 consisted of: 50 mM sodium phosphate, 150 mM NaCl in H_2O (pH 7.1); 50 mM sodium
230 phosphate, 150 mM NaCl in D_2O (pD 7.5); or 10-50 mM sodium phosphate, 2 M NaCl in D_2O
231 (pD 7.5). The reaction mixture was transferred to the polarimetry cell and after 5 min the
232 mutarotation rate was monitored continuously at 26±1 ºC by reading specific rotation at various
233 times. The rate constant was calculated using the Prism 6 software package (Graphpad
234 Scientific Software). Data were fitted to a one phase decay function, $t_{1/2} = \ln(2)/k$.

235 For mutarotation as described in equation 1, the rate of change in the concentration of
236 the α-anomer has two contributions: it is depleted by the forward reaction at rate $k_1[\alpha]$ and is
237 replenished by the reverse reaction at rate $k_{-1}[\alpha]$. The net rate of change is therefore:

238

239 $$\frac{d[\alpha]}{dt} = -k_1[\alpha] + k_{-1}[\beta] \quad (12)$$

240

241 The solution of this first-order differential equation is:

242

243 $$[\alpha] = \left\{\frac{k_{-1}+k_1 e^{-(k_1+k_{-1})t}}{k_1+k_{-1}}\right\}[\alpha]_0 \quad (13)$$

244

245 And thus the first order decay constant (k) is related to the forward and reverse rates as:

$$k = k_1 + k_{-1} \quad (14)$$

Using equation (5), which relates the equilibrium constant to the forward and reverse rates, this shows that:

$$K^{eq} = \frac{[\beta]^{eq}}{[\alpha]^{eq}} = \frac{k_1}{k - k_1} \quad (15)$$

Results

Our initial efforts to characterize SQ mutarotases focused on expressing *YihR* from *E. coli* (which utilizes the sulfo-EMP pathway) [1], and *PpSQ1_00415* from *P. putida* SQ1 (which utilizes the sulfo-ED pathway) [2] in an *E. coli* expression system. However, despite screening several expression constructs and conditions, only a poor yield of low quality protein was ever obtained. Thus, we turned our attention to other putative SQ mutarotases from various bacteria that possess sulfoglycolytic gene clusters and succeeded in obtaining WP_069374721.1 (hereafter *Hs*SQM) from *Herbaspirillum seropedicaea* in high yield and purity. *H. seropedicaea* is a nitrogen-fixing endophytic bacterium capable of colonizing the intercellular spaces of grasses such as rice and sugar cane [23], and contains a predicted sulfo-ED operon analogous to that of *P. putida* SQ1 but lacking in synteny (Figure 2A) [2]. A sequence alignment of these three putative sulfoquinovose mutarotases, as well as two structurally characterized hexose mutarotases, is provided in Figure 2B: *Hs*SQM shares 37% similarity (19% identity) with *E. coli* YihR, and 50% similarity (35% identity) with *P. putida* SQ1 PpSQ1_00415 (SI Table 1). All three proteins retain the highly conserved residues of other hexose mutarotases (His92, His162 and Glu254 in *Hs*SQM). The equivalent residue to *Hs*SQM His162 in galactose mutarotase from *E. coli* has previously been proposed to be involved in substrate binding [24], whereas the equivalent residues to His92 and Glu254 are proposed to act in roles of general acid and general base, respectively, in the first half of the reaction leading to the acyclic aldehyde, in galactose mutarotases from both *L. lactis* and *E. coli* [24, 25].

The iTASSER server [26-28] provided a homology model of *Hs*SQM with a C-score of 0.87, suggesting it to be a good approximation for the protein's native fold. This was compared to existing structures by using TM-align [29, 30] and returned only other (predicted) mutarotase structures. Greatest structural similarity was found between the *Hs*SQM model and

279 a galactose mutarotase-like protein from *Clostridium acetobutylicum* (PDB 3OS7, Figure 3A),
280 with a RMSD of 1.55 Å between structural models, despite both proteins sharing <15%
281 identity. Structural alignment of the *Hs*SQM homology model and the galactose mutarotase
282 domain of gal10 from *S. cerevisae* with D-galactose bound (PDB 1Z45) [31] reveals that the
283 conserved active site residues His92, His162 and Glu254 in the homology model are positioned
284 appropriately for catalysis (Figure 3B).

285 2D ^{1}H-^{1}H EXSY was used to assess whether *Hs*SQM can catalyze mutarotation. A 2D
286 pulse sequence equivalent to that used for a 2D ^{1}H-^{1}H NOESY experiment was employed to
287 provide a visual representation of the chemical exchange network [15, 20]. A similar approach
288 was utilized by Graille and coworkers to study a hexose-6-phosphate mutarotase [32], building
289 on work by Balaban and Ferretti for the study of anomerization/isomerization of Glc-6-P by
290 phosphoglucose isomerase using 2D ^{31}P-^{31}P EXSY [17], and earlier work by Kuchel and
291 coworkers, who studied mutarotation catalyzed by porcine mutarotase using ^{13}C-^{13}C EXSY
292 [16]. In this approach, all nuclei are excited using a 90° excitation pulse, which is allowed to
293 evolve over a t_1 period. A second 90° pulse is then applied to rotate the *y*-component of
294 magnetization onto the *z*-axis, and a mixing interval τ_{mix}, allows magnetization transfer through
295 chemical exchange. A final 90° pulse creates transverse magnetization in the *xy* plane, which
296 is detected. Molecules that undergo chemical interconversion display cross-peak signals
297 between a signal from the substrate along one axis of the 2D spectrum, and the corresponding
298 nucleus in the product on the other axis. Careful choice of mixing time to be shorter than that
299 required for chemical exchange by spontaneous mutarotation can allow qualitative detection
300 of enzyme-catalyzed mutarotation in a single NMR experiment. Figure 4A shows that a
301 solution of SQ displays H1 of the α- and β-anomers as independent sets of signals, and upon
302 addition of *Hs*SQM off-diagonal cross-peaks appear between the anomeric proteins. This data
303 provides evidence that chemical exchange is occurring and that *Hs*SQM is catalyzing the
304 mutarotation of SQ.

305 To qualitatively explore the substrate specificity of *Hs*SQM, we assessed the ability of
306 the enzyme to catalyze mutarotation of other simple hexoses (Figures 4B-F). *Hs*SQM could
307 catalyze the mutarotation of D-glucose-6-phosphate and D-glucuronic acid, showing that the
308 sulfonate group is not required and that *Hs*SQM can tolerate other anionic groups. A set of
309 simple aldohexoses was also studied. *Hs*SQM catalyzed mutarotation of D-glucose and D-
310 galactose, showing that the enzyme is tolerant of either stereochemistry at C4. However, using
311 this pulse sequence we could not detect *Hs*SQM-mediated mutarotation of D-mannose on the

312 NMR time-scale, demonstrating the preference of *Hs*SQM for substrates with an equatorial
313 C2-hydroxyl group.
314 While these experiments provide insights into the substrate specificity of *Hs*SQM,
315 simple hexoses are not present at any appreciable concentration within bacterial cells, as shown
316 for *E. coli* grown on various carbon sources [33]. Other than SQ, the only other physiologically
317 plausible substrate for *Hs*SQM is glucose-6-phosphate (Glc-6-P): an abundant primary
318 metabolite produced by bacteria grown on glucose, glycerol or acetate [33]. To explore the
319 selectivity of *Hs*SQM for SQ and Glc-6-P, we used EXSY to determine kinetic parameters
320 under conditions of equilibrium exchange. While it is possible to use 2D methods to determine
321 rates, accurate determination requires *a priori* knowledge of optimum mixing times and a
322 lengthy experiment, and so we elected to use the alternative 1D EXSY approach. Measurement
323 of the equilibrium-exchange rate constants was achieved by selective inversion of a distinctive
324 signal from one anomer and then monitoring the return to equilibrium intensity of signals from
325 both anomers. For quantitative determination of rates, the selective irradiation must be of
326 sufficient power and duration to invert the targeted magnetization, yet should not directly affect
327 the equilibrium magnetization of the other spin population. Due to the chemical exchange of
328 the anomers, the inverted magnetization redistributes into the un-irradiated site. The
329 magnetization can then be sampled by normal methods. Figures 5A,B show build-up curves of
330 H1α arising from the irradiation of H1β of SQ and Glc-6-P, respectively; and Figures 5C,D
331 show the respective decay curves from the same experiment for H1β. Also shown is the tangent
332 at $\tau_{mix} = 0$, which provides the exchange-rate constant. Figures 5E,F show Michaelis-Menten
333 plots for conversion of the β-anomers of SQ and Glc-6-P, respectively. While SQ exhibited
334 saturation kinetics, allowing calculation of k_{cat}, K_M and k_{cat}/K_M values, Glc-6-P did not and thus
335 only k_{cat}/K_M could be calculated. As the equilibrium concentrations of the two anomers of each
336 substrate are known, this data allows calculation of kinetic parameters for the reverse reaction.
337 The complete set of kinetic parameters for the forward and reverse mutarotation reactions are
338 shown in Table 1, and reveals that *Hs*SQM displays an approximate 5-fold selectivity for SQ
339 over Glc-6-P in terms of the k_{cat}/K_M values.
340
341 **Table 1.** Michaelis Menten kinetic parameters for *Hs*SQM catalyzed mutarotation of SQ and
342 Glc-6-P under conditions of equilibrium exchange.

substrate	k_{cat} **(s^{-1})**	K_M **(mM)**	k_{cat}/K_M **(M^{-1} s^{-1})**
α-SQ	$(3.08\pm0.19) \times 10^2$	1.00±0.20	$(3.07\pm0.44) \times 10^5$

β-SQ	(3.37±0.20) × 10^2	2.08±0.34	(1.62±0.18) × 10^5
α-Glc-6-P	–	–	(5.87±0.57) × 10^4
β-Glc-6-P	–	–	(3.26±0.31) × 10^4

To gain insight into the rate enhancement achieved by *Hs*SQM we measured the rate of mutarotation of SQ by polarimetry using a coupled assay. Incubation of 4-nitrophenyl α-D-sulfoquinovoside with a retaining sulfoquinovosidase occurs with retention of configuration to afford α-SQ. Monitoring the rate of mutarotation of α-SQ in 50 mM phosphate buffer revealed a half-life of 50 min (SI Figure 1). By comparison, mutarotation of α-Glc-6-P has been reported to occur at 25 °C with a half-life of 6.0 s [34, 35]. However, phosphate buffer is known to catalyze mutarotation.[36] In order to measure the rate of mutarotation in phosphate-free conditions, and to subsequently allow comparison with enzyme-catalyzed rates measured in D_2O we measured mutarotation rates of SQ in D_2O at various concentrations of phosphate at pseudo-constant ionic strength achieved with 2 M NaCl (Figure 6A). Extrapolation of this data to [phosphate] = 0 mM, gave a predicted mutarotation rate (k) of 3.87×10^{-5} s^{-1} (0.00232 min^{-1}) corresponding to a half-life of 299 min. Using the equilibrium constant $K^{eq} = 1.5$ allows calculation of forward and reverse rates of $k_1 = 2.3 \times 10^{-5}$ s^{-1} and $k^{-}_1 = 1.5 \times 10^{-5}$ s^{-1}. A similar calculation for Glc-6-P mutarotation ($K^{eq} = 1.8$) using the published data gave forward and reverse rates of $k_1 = 7.7 \times 10^{-2}$ s^{-1} and $k_{-1} = 4.3 \times 10^{-2}$ s^{-1}; strictly speaking these 'uncatalyzed' rates are for $k_{(H2O)} + k_{(H+)}[H_3O^+] + k_{(HO-)}[HO^-]$.

The above data allow us to calculate the catalytic proficiency of *Hs*SQM for catalyzing the mutarotation of SQ and Glc-6-P. The proficiency constants [k_{uncat} / (k_{cat}/K_M)] for *Hs*SQM are 7.6×10^{-11} M for α-SQ and 1.3×10^{-6} M for α-Glc-6-P, revealing that *Hs*SQM binds the SQ transition state some 17,000-fold tighter than for Glc-6-P and is thus best considered a sulfoquinovose mutarotase. We note that the mutarotation rate for Glc-6-P was measured in H_2O, whereas all other measurements were performed in D_2O, thus a solvent isotope effect may somewhat confound this analysis; nonetheless the broad conclusions still apply.

The pD dependence of activity for *Hs*SQM was determined using 1D ^{1}H EXSY for Glc-6-P. At a concentration of 5 mM, Glc-6-P does not show saturation (unlike for SQ), and so rates measured at this concentration provide an estimate of k_{cat}/K_M. Figure 6 shows the pD dependence of activity is bell-shaped, with a broad maximum of activity of pD 7-9. The simplest interpretation of these results is that it arises from ionization of two catalytically important residues with pK_a values of 6.3±0.2 and 10.3±0.2. The ionization of the acidic limb

373 presumably reflections ionization of the general acid Glu254, and the basic limb ionization of
374 the general base His92. By comparison, the intrinsic pK_a values for the ionizable side-chains
375 of Glu and His are 4.5 and 6.4, respectively [37]. In both cases, and particularly the latter, these
376 intrinsic pK_a values are perturbed, presumably because of the active-site environment including
377 charge-charge and charge-dipole interactions, as well as desolvation effects [37]. The pD
378 dependence of this enzyme is similar to the pH dependence of green pepper mutarotase [34],
379 but broader than that of *E. coli* galactose mutarotase [38].
380
381 **Discussion**
382 Many enzymes involved in the metabolism of free sugars are stereospecific for one anomer of
383 their substrate. For example, yeast galactokinase specifically phosphorylates α-galactose to
384 produce α-D-galactose-1-phosphate [39], glucose dehydrogenase from *Bacillus megaterium*
385 uses only β-D-glucose as a substrate [40]; yeast phosphoglucose isomerase only uses α-D-
386 glucose-6-phosphate as substrate [41]; and yeast phosphomannose isomerase is specific for α-
387 D-mannose-6-phosphate [42]. For these enzymes, access to the appropriate substrate anomer
388 would be rate-limiting *in vivo* if the process relied on spontaneous mutarotation. Mutarotases
389 ensure that there is rapid equilibration between anomers to eliminate this metabolic bottleneck.
390 While some mutarotases have been linked to specific metabolic pathways [6], it has been
391 difficult to assign many others to a single substrate or metabolic process [32]. It is unclear if
392 the inherent promiscuity of many mutarotases confers an advantage to their hosts or simply
393 impose no cost to fitness.
394 Sulfo-EMP and sulfo-ED gene clusters both encode putative mutarotases, homologous
395 to *Hs*SQM, that are upregulated in response to growth on SQ [1, 2], suggesting that their
396 primary function is as an SQ mutarotase. We show here that *Hs*SQM from the sulfo-ED cluster
397 of *H. seropedicaea* can catalyze SQ mutarotation with a greater k_{cat}/K_M value than for the
398 possible alternative substrate Glc-6-P, which is itself an important metabolite that feeds into
399 the Embden-Meyerhof-Parnas and Entner-Doudoroff glycolytic pathways, as well as the
400 pentose phosphate pathway. It is possible that the activity of the enzyme on Glc-6-P is
401 advantageous to a bacterium transitioning between growth on SQ and growth on Glc.
402 Furthermore, due to the broad substrate tolerance of many mutarotases, it is possible that other
403 enzymes may play a role in catalysing SQ mutarotation within the cell, though any enzyme
404 that does so is unlikely to be transcriptionally regulated by SQ concentration as *Hs*SQM and
405 its homologs are.

The substrate specificity of *Hs*SQM bears similarities to the aldose-1-epimerase from *E. coli* (galM), which is tolerant to functional group changes at C6, and stereochemistry changes at C4 (Gal) but not at C2 (Man) [9]. On the other hand it is distinguished from yeast ymr099c, which encodes a hexose-6-phosphate mutarotase with activity on Glc-6-P, Gal-6-P and Man-6-P and thus tolerates stereochemical inversion at C2 [32]. Sequence alignments and structural modelling reveal that *Hs*SQM likely acts through a mechanism conserved with all other mutarotases. The substrate tolerance of *Hs*SQM for substituent variation at C6 lies in contrast to *E. coli* SQase, which exhibited negligible activity on α-glucosides due to its specialized set of conserved residues that recognize the sulfonate group of SQ glycosides [4].

The effectiveness of an enzyme as a catalyst can be quantified by measuring the rate enhancement it provides relative to the rate of the uncatalyzed reaction [43]. This work reveals that uncatalyzed SQ mutarotation is a relatively slow reaction, with the rate for α-SQ some 3400-fold lower than that of α-Glc-6-P. On the other hand, *Hs*SQM catalyzes mutarotation with a k_{cat}/K_M value around 5-fold higher than for Glc-6-P. Combining these values reveals that *Hs*SQM is approximately 17,000-fold more proficient as a catalyst in catalyzing the mutarotation of SQ and Glc-6-P. As enzymes achieve their rate enhancement through selective stabilization of the transition state relative to the ground state, these data suggest that the affinity for the transition state of SQ mutarotation is approximately 17,000-fold greater than that for Glc-6-P mutarotation. As has been noted by others, the unusually high rate of mutarotation of Glc-6-P is much greater than that of other hexoses [44], and appears to be a result of neighboring group participation by the pendant phosphate group [36]; our data suggests that the sulfonate group of SQ does not provide neighbouring group participation.

Understanding the precise role of SQMs in the sulfo-EMP and sulfo-ED pathways will require knowledge of the substrate specificities for upstream and downstream processes. Upstream processes include SQ importers and SQases. For organisms grown on a mixture of SQ anomers, the SQ importers may exhibit a preference for only one SQ anomer; an SQM may be required for re-establishing an equilibrium mixture of SQ anomers. A pertinent example is that of red blood cells in which it is known that glucose importers exhibit a preference for α-glucose [45], and a potential role for glucomutarotase in a permease system involved in re-establishing this equilibrium has been advanced [34]. For cells grown on SQ glycosides, SQ is released by action of SQases; the immediate product is α-SQ, and SQMs may be required to enhance conversion of α-SQ to β-SQ, to match the preference of a downstream enzyme, or to act in the reverse direction to 'rescue' β-SQ that accumulates as a result of the spontaneous

mutarotation of α-SQ. Downstream enzymes include SQ isomerases and SQ dehydrogenases. As yet the anomeric preference, if any, of these enzymes is unknown. The NMR EXSY experiments used herein to probe SQM activity, which build on pioneering work reaching back many decades, could be of use for studying the substrate preferences of the downstream enzymes, and in so doing could help provide the biological context for the SQMs.

Abbreviations

DHAP, dihydroxyacetone phosphate; DHPS, 2,3-dihydroxypropanesulfonate; Gal, galactose; Glc, glucose; GlcA, glucuronic acid; Man, mannose; ED, Entner-Doudoroff; EMP, Embden-Meyerof-Parnas; EXSY, exchange spectroscopy; NMR, nuclear magnetic resonance; PNPSQ, 4-nitrophenyl α-D-sulfoquinovoside; SL, sulfolactate; SQ, sulfoquinovose; SQase, sulfoquinovosidase; SQM, sulfoquinovose mutarotase.

Author Contribution

S.J.W., S.Y. and E.D.G-B. conceived and coordinated the study. J.P.L. and J.Y. performed the cloning and protein expression. P.A. and S.Y. conducted the NMR measurements. P.A. and C.B. conducted the polarimetry measurements. All authors contributed to writing of the manuscript and approved the final version of the manuscript.

Funding

We thank the Australian Research Council for funding (DP180101957). GJD is a Royal Society Ken Murray Research Fellow and sulfoquinovose work in York is supported by the Leverhulme Trust. EDG-B acknowledges support from the Australian Cancer Research Foundation, Victorian State Government Operational Infrastructure Support and Australian Government NHMRC IRIISS.

Acknowledgements

We thank Prof Frances Separovic for suggesting the use of EXSY to study this system.

Competing Interests

The Authors declare that there are no competing interests associated with the manuscript.

References

1 Denger, K., Weiss, M., Felux, A. K., Schneider, A., Mayer, C., Spiteller, D., Huhn, T., Cook, A. M. and Schleheck, D. (2014) Sulphoglycolysis in *Escherichia coli* K-12 closes a gap in the biogeochemical sulphur cycle. Nature. **507**, 114-117

2 Felux, A. K., Spiteller, D., Klebensberger, J. and Schleheck, D. (2015) Entner-Doudoroff pathway for sulfoquinovose degradation in *Pseudomonas putida* SQ1. Proc. Natl. Acad. Sci. USA. **112**, E4298-4305

3 Goddard-Borger, E. D. and Williams, S. J. (2017) Sulfoquinovose in the biosphere: occurrence, metabolism and functions. Biochem. J. **474**, 827–849

4 Speciale, G., Jin, Y., Davies, G. J., Williams, S. J. and Goddard-Borger, E. D. (2016) YihQ is a sulfoquinovosidase that cleaves sulfoquinovosyl diacylglyceride sulfolipids. Nat. Chem. Biol. **12**, 215-217

5 Tanner, M. (1997) Mutarotases. In Comprehensive Biological Catalysis (Sinnott, M. L., ed.). pp. 208-209, Academic Press, London

6 Holden, H. M., Rayment, I. and Thoden, J. B. (2003) Structure and function of enzymes of the Leloir pathway for galactose metabolism. J. Biol. Chem. **278**, 43885-43888

7 Levy, G. B. and Cook, E. S. (1954) A rotographic study of mutarotase. Biochem. J. **57**, 50-55

8 Keston, A. S. (1964) A sensitive polarimetric assay of mutarotase utilizing racemic mixtures of sugars. Anal. Biochem. **9**, 228-242

9 Hucho, F. and Wallenfels, K. (1971) The enzymatically catalyzed mutarotation. The mechanism of action of mutarotase (aldose 1-epimerase) from *Escherichia coli*. Eur. J. Biochem. **23**, 489-496

10 Okuda, J., Miwa, I., Maeda, K. and Tokui, K. (1977) Rapid and sensitive, colorimetric determination of the anomers of D-glucose with D-glucose oxidase, peroxidase, and mutarotase. Carbohydr. Res. **58**, 267-270

11 Hill, J. B. and Cowart, D. S. (1966) An automated colorimetric mutarotase assay. Anal. Biochem. **16**, 327-337

12 Weibel, M. K. (1976) A coupled enzyme assay for aldose 1-epimerase. Anal. Biochem. **70**, 489-494

13 Bentley, R. and Bhate, D. S. (1960) Mutarotase from *Penicillium notatum*. I. Purification, assay, and general properties of the enzyme. J. Biol. Chem. **235**, 1219-1224

14 Kuchel, P. W. (1990) Spin-exchange NMR spectroscopy in studies of the kinetics of enzymes and membrane transport. NMR Biomed. **3**, 102-119

15 Gaede, H. C. (2007) NMR exchange spectroscopy. In Modern NMR Spectroscopy in Education. pp. 176-189, American Chemical Society

16 Kuchel, P. W., Bulliman, B. T. and Chapman, B. E. (1988) Mutarotase equilibrium exchange kinetics studied by ^{13}C-NMR. Biophys. Chem. **32**, 89-95

17 Balaban, R. S. and Ferretti, J. A. (1983) Rates of enzyme-catalyzed exchange determined by two-dimensional NMR: a study of glucose 6-phosphate anomerization and isomerization. Proc. Natl. Acad. Sci. USA. **80**, 1241-1245

18 Ryu, K. S., Kim, C., Park, C. and Choi, B. S. (2004) NMR analysis of enzyme-catalyzed and free-equilibrium mutarotation kinetics of monosaccharides. J. Am. Chem. Soc. **126**, 9180-9181

19 Ryu, K. S., Kim, C., Kim, I., Yoo, S., Choi, B. S. and Park, C. (2004) NMR application probes a novel and ubiquitous family of enzymes that alter monosaccharide configuration. J. Biol. Chem. **279**, 25544-25548

518 20 Perrin, C. L. and Dwyer, T. J. (1990) Application of two-dimensional NMR to kinetics
519 of chemical exchange. Chem. Rev. **90**, 935-967
520 21 Aski, S. N., Takacs, Z. and Kowalewski, J. (2008) Inclusion complexes of cryptophane–
521 E with dichloromethane and chloroform: A thermodynamic and kinetic study using the 1D-
522 EXSY NMR method. Magn. Res. Chem. **46**, 1135-1140
523 22 Kumar, A., Wagner, G., Ernst, R. R. and Wuethrich, K. (1981) Buildup rates of the
524 nuclear Overhauser effect measured by two-dimensional proton magnetic resonance
525 spectroscopy: implications for studies of protein conformation. J. Am. Chem. Soc. **103**, 3654-
526 3658
527 23 Baldani, J. I., Baldani, V. L. D., Seldin, L. and Döbereiner, J. (1986) Characterization of
528 *Herbaspirillum seropedicae* gen. nov., sp. nov., a root-associated nitrogen-fixing bacterium.
529 Int. J. Syst. Evolutionary Microbiol. **36**, 86-93
530 24 Beebe, J. A. and Frey, P. A. (1998) Galactose mutarotase: purification,
531 characterization, and investigations of two important histidine residues. Biochemistry. **37**,
532 14989-14997
533 25 Thoden, J. B., Kim, J., Raushel, F. M. and Holden, H. M. (2002) Structural and kinetic
534 studies of sugar binding to galactose mutarotase from *Lactococcus lactis*. J. Biol. Chem. **277**,
535 45458-45465
536 26 Yang, J., Yan, R., Roy, A., Xu, D., Poisson, J. and Zhang, Y. (2015) The I-TASSER Suite:
537 protein structure and function prediction. Nat. Methods. **12**, 7-8
538 27 Roy, A., Kucukural, A. and Zhang, Y. (2010) I-TASSER: a unified platform for
539 automated protein structure and function prediction. Nat. Protoc. **5**, 725-738
540 28 Zhang, Y. (2008) I-TASSER server for protein 3D structure prediction. BMC
541 Bioinformatics. **9**, 40
542 29 Zhang, Y. and Skolnick, J. (2004) Scoring function for automated assessment of
543 protein structure template quality. Proteins. **57**, 702-710
544 30 Xu, J. and Zhang, Y. (2010) How significant is a protein structure similarity with TM-
545 score = 0.5? Bioinformatics. **26**, 889-895
546 31 Thoden, J. B. and Holden, H. M. (2005) The molecular architecture of galactose
547 mutarotase/UDP-galactose 4-epimerase from *Saccharomyces cerevisiae*. J. Biol. Chem. **280**,
548 21900-21907
549 32 Graille, M., Baltaze, J. P., Leulliot, N., Liger, D., Quevillon-Cheruel, S. and van
550 Tilbeurgh, H. (2006) Structure-based functional annotation: yeast ymr099c codes for a D-
551 hexose-6-phosphate mutarotase. J. Biol. Chem. **281**, 30175-30185
552 33 Bennett, B. D., Kimball, E. H., Gao, M., Osterhout, R., Van Dien, S. J. and Rabinowitz,
553 J. D. (2009) Absolute metabolite concentrations and implied enzyme active site occupancy
554 in Escherichia coli. Nat. Chem. Biol. **5**, 593-599
555 34 Bailey, J. M., Fishman, P. H. and Pentchev, P. G. (1967) Studies on mutarotases. I.
556 Purification and properties of a mutarotase from higher plants. J. Biol. Chem. **242**, 4263-
557 4269
558 35 Bailey, J. M., Pentchev, P. G. and Fishman, P. H. (1967) A study of rate limiting
559 anomerizations in glucose metabolism. Fed. Proc. **26**, 854
560 36 Bailey, J. M., Fishman, P. H. and Pentchev, P. G. (1970) Anomalous mutarotation of
561 glucose 6-phosphate. An example of intramolecular catalysis. Biochemistry. **9**, 1189-1194
562 37 Harris, T. K. and Turner, G. J. (2002) Structural basis of perturbed pKa values of
563 catalytic groups in enzyme active sites. IUBMB Life. **53**, 85-98

564 38 Beebe, J. A., Arabshahi, A., Clifton, J. G., Ringe, D., Petsko, G. A. and Frey, P. A. (2003)
565 Galactose mutarotase: pH dependence of enzymatic mutarotation. Biochemistry. **42**, 4414-
566 4420
567 39 Howard, S. M. and Heinrich, M. R. (1965) The anomeric specificity of yeast
568 galactokinase. Archiv. Biochem. Biophys. **110**, 395-400
569 40 Pauly Hans, E. and Pfleiderer, G. (1975) D-Glucose dehydrogenase from *Bacillus*
570 *megaterium* M 1286: Purification, properties and structure. Hoppe-Seylers Z. Physiol. Chem.
571 **356**, 1613
572 41 Willem, R., Malaisse-Lagae, F., Ottinger, R. and Malaisse, W. J. (1990)
573 Phosphoglucoisomerase-catalysed interconversion of hexose phosphates. Kinetic study by
574 ^{13}C n.m.r. of the phosphoglucoisomerase reaction in $^{2}H_2O$. Biochem. J. **265**, 519-524
575 42 Rose, I. A., O'Connell, E. L. and Schray, K. J. (1973) Mannose 6-phosphate: anomeric
576 form used by phosphomannose isomerase and its 1-epimerization by phosphoglucose
577 isomerase. J. Biol. Chem. **248**, 2232-2234
578 43 Wolfenden, R. and Snider, M. J. (2001) The depth of chemical time and the power of
579 enzymes as catalysts. Acc. Chem. Res. **34**, 938-945
580 44 Salas, M., Vinuela, E. and Sols, A. (1965) Spontaneous and enzymatically catalyzed
581 anomerization of glucose 6-phosphate and anomeric specificity of related enzymes. J. Biol.
582 Chem. **240**, 561-568
583 45 Faust, R. G. (1960) Monosaccharide penetration into human red blood cells by an
584 altered diffusion mechanism. J. Cell. Comp. Physiol. **56**, 103-121
585

586

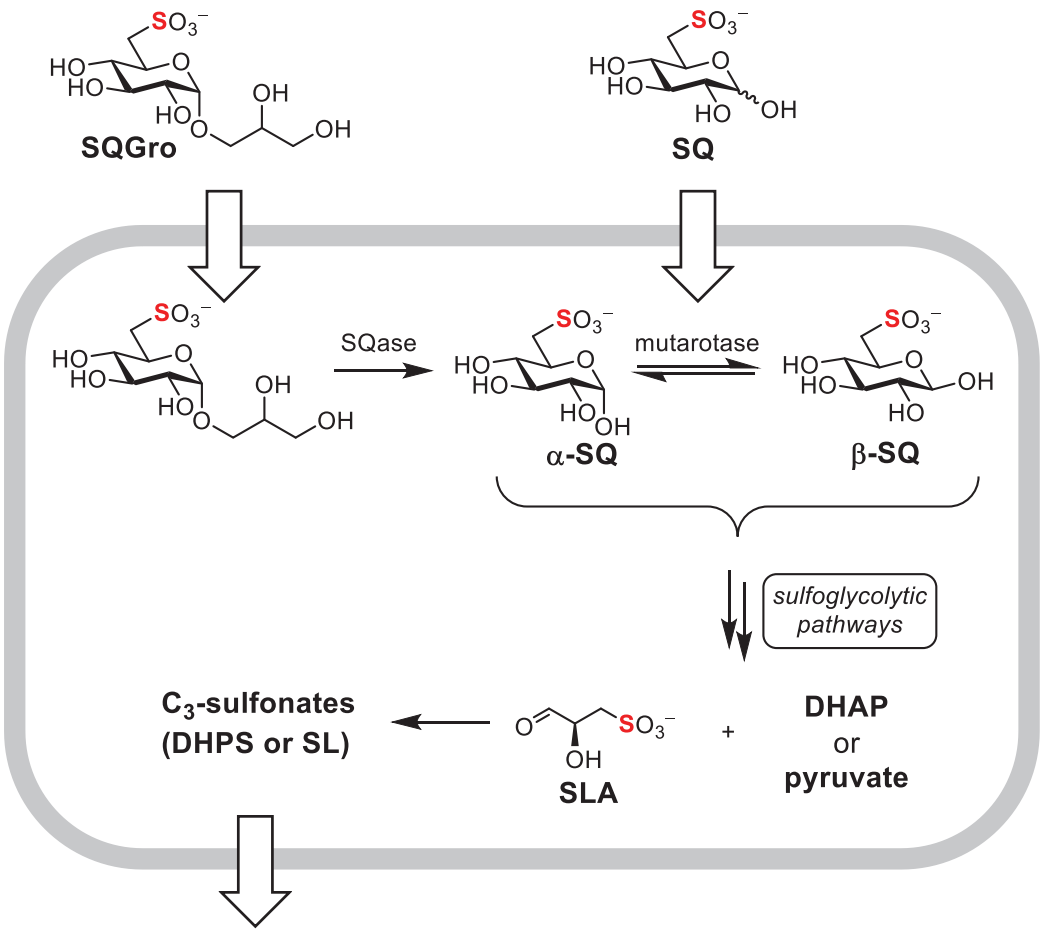

587

588 **Figure 1. Summary of sulfoglycolysis.**

589 Importation of SQGro and cleavage by SQase, or direct importation of SQ, provides an
590 intracellular pool of SQ anomers that can be interconverted by SQ mutarotase. SQ is
591 metabolized by sulfo-ED or sulfo-EMP pathways to sulfolactaldehyde (SLA), and then to the
592 C_3-sulfonates dihydroxypropanesulfonate (DHPS) or sulfolactate (SL), prior to export.

593

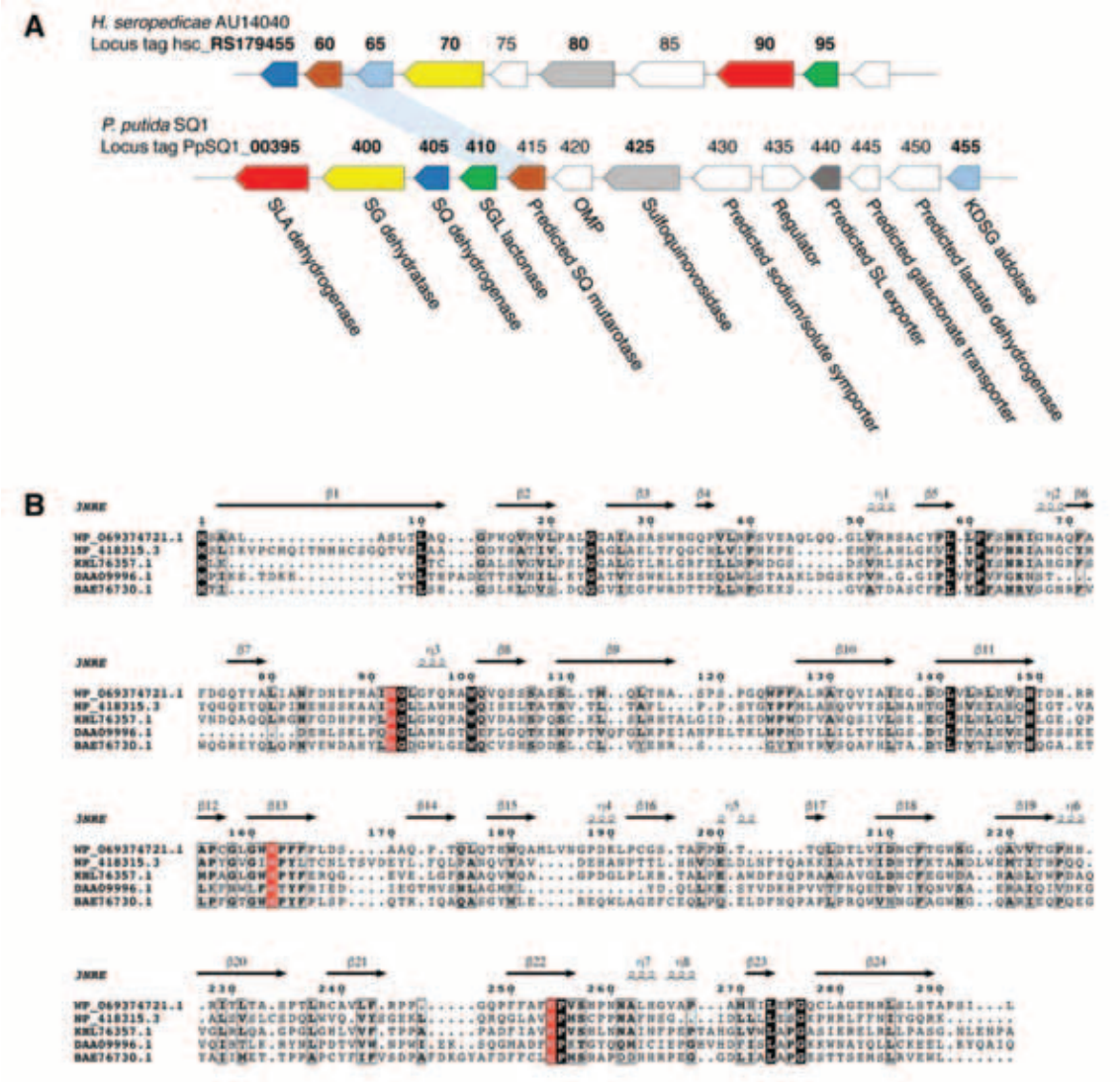

Figure 2. *Herbaspirillum seropedicaea* contains a sulfo-ED operon and a putative SQ mutarotase.

A) Operon structure of *P. putida* SQ1 and *H. seropedicaea* strain AU14040. Bold indicates genes for which enzymatic activity has been biochemically determined in at least one organism. B) Alignment of various putative mutarotases with secondary structural elements. WP_069374721.1, HsQM from *H. seropedicaea*; NP_418315.3, YihQ from *E. coli*; KHL76357.1, PpSQ1_00415 from *Pseudomonas putida* SQ1; DAA09996.1, YMR099C hexose-1-phosphate mutarotase from *S. cerevisiae*; BAE76730.1, YphB aldose-1-epimerase from *E. coli* (BAE76730.1). The secondary structural elements are annotated from the structure of *E. coli* YphB (PDB 3nre).

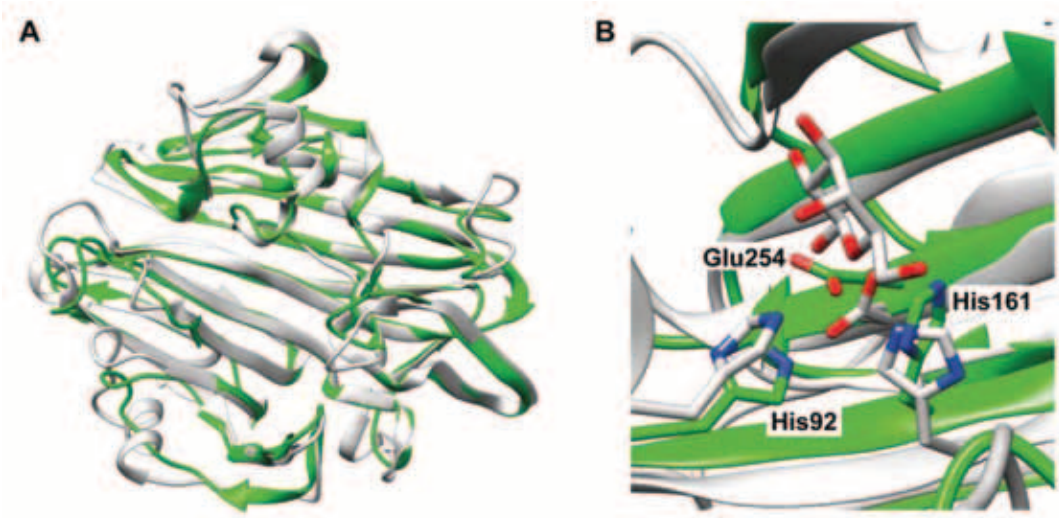

Figure 3. Homology model of *Hs*SQM.

A) Overlay of *Hs*SQM homology model (green) with a putative mutarotase from *Clostridium acetobutylicum* (PDB 3OS7; grey). B) The active sites of the *Hs*SQM homology model (green) overlaid with the galactose mutarotase domain of gal10 from *S. cerevisae* with D-galactose bound (grey, PDB 1Z45). Residue numbers are for *Hs*SQM.

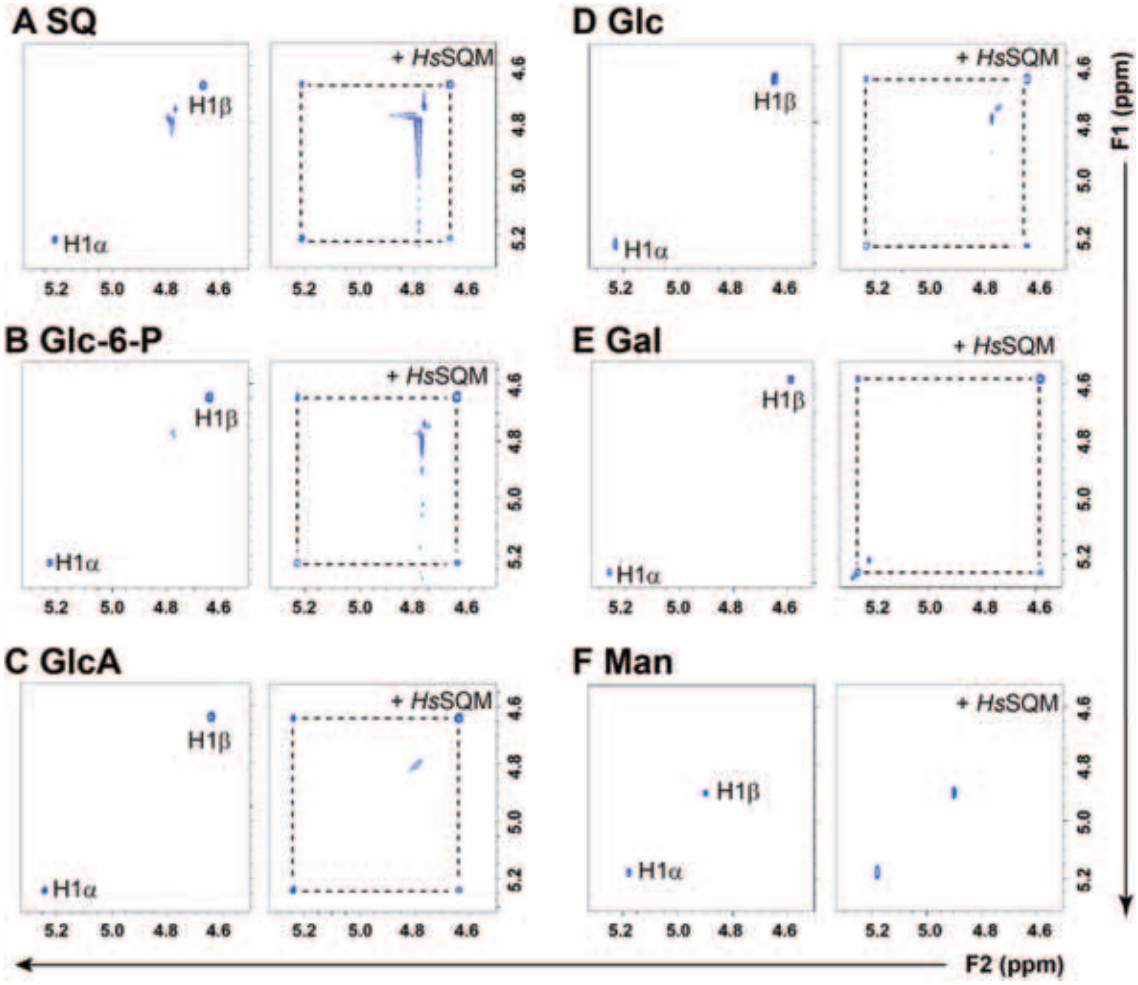

Figure 4. Excerpt showing anomeric regions of 2D ^{1}H-^{1}H EXSY plots of various hexoses alone and with *H. seropediacae* mutarotase.

A) sulfoquinovose (SQ), B) D-glucose-6-phosphate (Glc-6-P), C) D-glucuronic acid (GlcA), D) D-glucose (Glc), E) D-galactose (Gal), F) D-mannose (Man). Hexoses are at 5 mM, 1.51 µM *Hs*SQM in 50 mM sodium phosphate, 150 mM NaCl (pD 7.5).

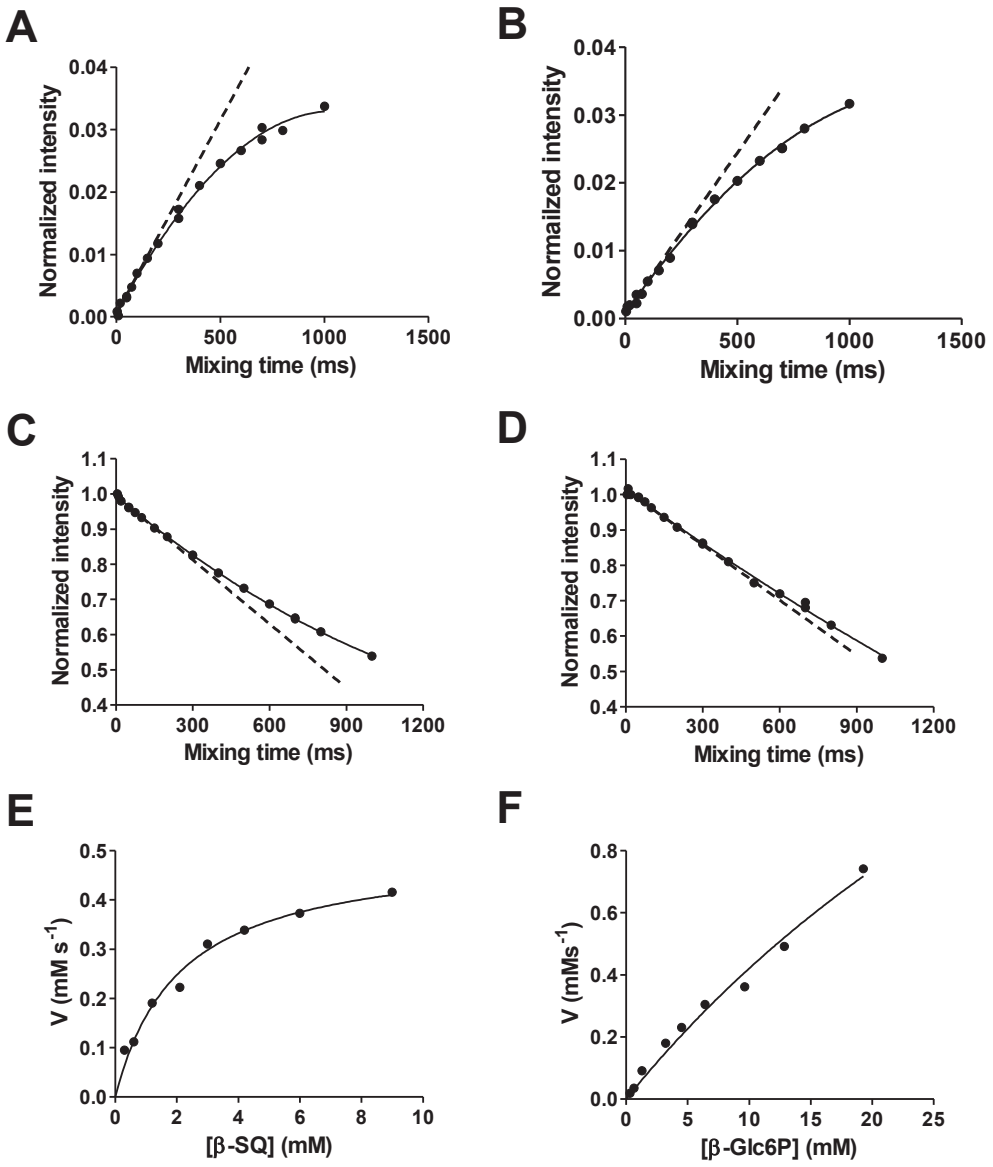

619
620

621 **Figure 5. Kinetic analysis of *Hs*SQM by inversion-recovery 1D ^{1}H EXSY.**

622 Inversion recovery curves for 10 mM SQ or Glc-6-P corresponding to (A) α-SQ at 4.00 mM
623 and (B) α-Glc-6-P at 3.57 mM. Inversion decay curves corresponding to (C) β-SQ at 6.00 mM
624 and (D) β-Glc-6-P at 6.43 mM. Michaelis-Menten plots for (E) β-SQ and (F) β-Glc-6-P.
625 Dashed lines indicate tangents to fitted curve at $t = 0$.

626

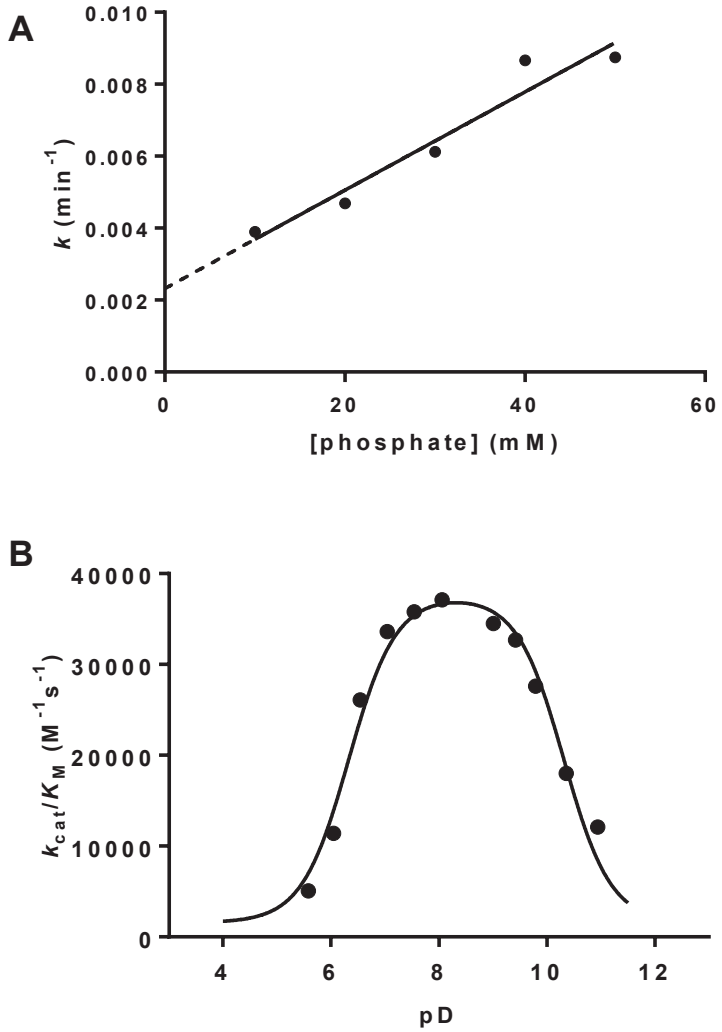

Figure 6. Spontaneous mutarotation of α-SQ and pD dependence of *Hs*SQM. A) Plot of rates of spontaneous mutarotation of α-SQ versus phosphate buffer concentration at pseudo-constant ionic strength. Buffers consisted of 10-50 mM sodium phosphate, 2 M NaCl in D_2O (pD 7.5). For comparison, $k = 0.0073$ min^{-1} in 50 mM sodium phosphate, 150 mM NaCl in D_2O (pD 7.5). B) pD dependence of *Hs*SQM activity for mutarotation of glucose-6-phosphate. Data was fit to a bell-shaped curve leading to estimated pK_a values of 5.9±0.1 and 9.9±0.1.

SUPPORTING INFORMATION

Discovery and characterization of a sulfoquinovose mutarotase using kinetic analysis at equilibrium by exchange spectroscopy

Palika Abayakoon, James P. Lingford, Yi Jin, Christopher Bengt, Gideon J. Davies, Shenggen Yao,* Ethan D. Goddard-Borger,* Spencer J. Williams*

Contents

*Hs*SQM plasmid and sequence data

plasmid	resistance	details
pET29-HsSQM	Kan	C-terminal His_6-tagged *Herbaspirillum seropedicae* strain AU14040 sulfoquinovose mutarotase (WP_069374721.1)

pET29-HsSQM

CDS:

```
ATGTCGGCAGCTCTTGCGTCCCTGACACTTGCCCAAGGACCGTGGCAAGTGCGCGTGCTGCCTGCACTGGGCGGTGCGATTGC
AAGCGCCAGCTGGCGTGGTCAGCCGGTGCTGCGCCCGAGCGTCGAGGCACAGCTGCAGCAGGGCCTGGTTAGACGCTCTGCGT
GCTATCCGCTGCTGCCGTTTAGTAACCGTATCGGAAACGCGCAATTCGCCTTTGATGGCCAGACATACGCGCTGATTGCCAAC
TTTGACAACGAACCGCACGCTATCCACGGGCTGGGCTTTCAGCGCGCGTGGCAGGTTCAGTCTAGCTCGGCGGAAAGTCTTAC
TATGCAGCTCACCCACGCCTCGCCGAGCCCGGGTCAGTGGCCGTTTGCCTTGCGTGCCACCCAGGTGATTGCCATCGAAGGCG
ACGATCTGGTGCTGCGCCTGGAAGTGGAAAATACCGATCATCGCCGCGCCCCATGCGGCCTGGGCTGGCATCCGTTTTTTCCG
CTGGATAGCGCGGCGCAGCCGACCCAGCTGCAGACCCATTGGCAAGCGATGCTGGTAAACGGGCCAGACAAACTTCCGTGCGG
CAGCACGGCCCCTCCGGATACGACCCAACTGGATACCTTAGTGATTGATAATTGCTTTACCGGCTGGAGCGGCCAGGCCGTCG
TTACCGGCCCGCATCATCGTATTACCCTGACAGCGAGCCCGACCCTGCGTTGCGCGGTGCTGTTTCGCCCGCCGGGGCAGCCG
TTCTTCGCGTTTGAACCGGTGAGCCATCCGAACAATGCCCTGCACGGCGTTGCGCCGGCGATGCACATCCTGGAACCCGGTCA
GTGCCTGGCGGGCGAAATGCGCCTGAGCCTGTCGACCGCTCCGAGCATTCTGGCGGCCGCACTCGAGCACCACCACCACCACC
ACTGA
```

Translation:

```
MSAALASLTLAQGPWQVRVLPALGGAIASASWRGQPVLRPSVEAQLQQGLVRRSACYPLL
PFSNRIGNAQFAFDGQTYALIANFDNEPHAIHGLGFQRAWQVQSSSAESLTMQLTHASPS
PGQWPFALRATQVIAIEGDDLVLRLEVENTDHRRAPCGLGWHPFFPLDSAAQPTQLQTHW
QAMLVNGPDKLPCGSTAPPDTTQLDTLVIDNCFTGWSGQAVVTGPHHRITLTASPTLRCA
VLFRPPGQPFFAFEPVSHPNNALHGVAPAMHILEPGQCLAGEMRLSLSTAPSILAAALEH
HHHHH*
```

Table S1. Pairwise sequence comparisons of HsSQM with various hexose mutarotases.*

H. seropediaceae	*P. putida*	*E. coli*	*L. lactis*	*S. cerevisiae*	
***Hs*SQM** WP_069374721.1	**PpSQ_00415** KHL76357.1	**YihQ** NP_418315.3	**GalM** WP_039116219.1	**YMR099C** DAA09996.1	**% identity (%similarity)**
	35 (49)	19 (38)	13 (26)	13 (28)	**HsSQM**
		19 (37)	12 (24)	15 (29)	**PpSQ_00415**
			12 (29)	11 (23)	**YihQ**
				14 (23)	**GalM**
					YMR099C

* Calculated using the "Sequence Manipulation Suite" and the following groupings of similar amino acids: GAVLI, FYW, CM, ST, KRH, DENQ, P.

See: http://www.bioinformatics.org/sms2/ident_sim.html, Stothard, P. *Biotechniques*, 2000, 28, 1102–1104.

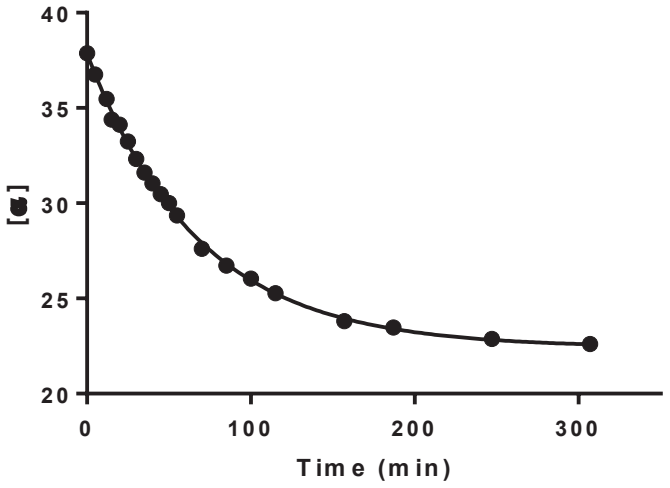

Figure S1. Mutarotation of SQ monitored by polarimetry.

4-Nitrophenyl α-D-sulfoquinovoside in 50 mM sodium phosphate, 150 mM NaCl in H_2O (pH 7.1) was treated with sulfoquinovosidase, and after 5 min, the specific rotation was monitored as a function of time. pH 7.1, 26±1 °C.

1D ^{1}H NMR spectra

Sulfoquinovose (600 MHz, 15 mM, D_2O)

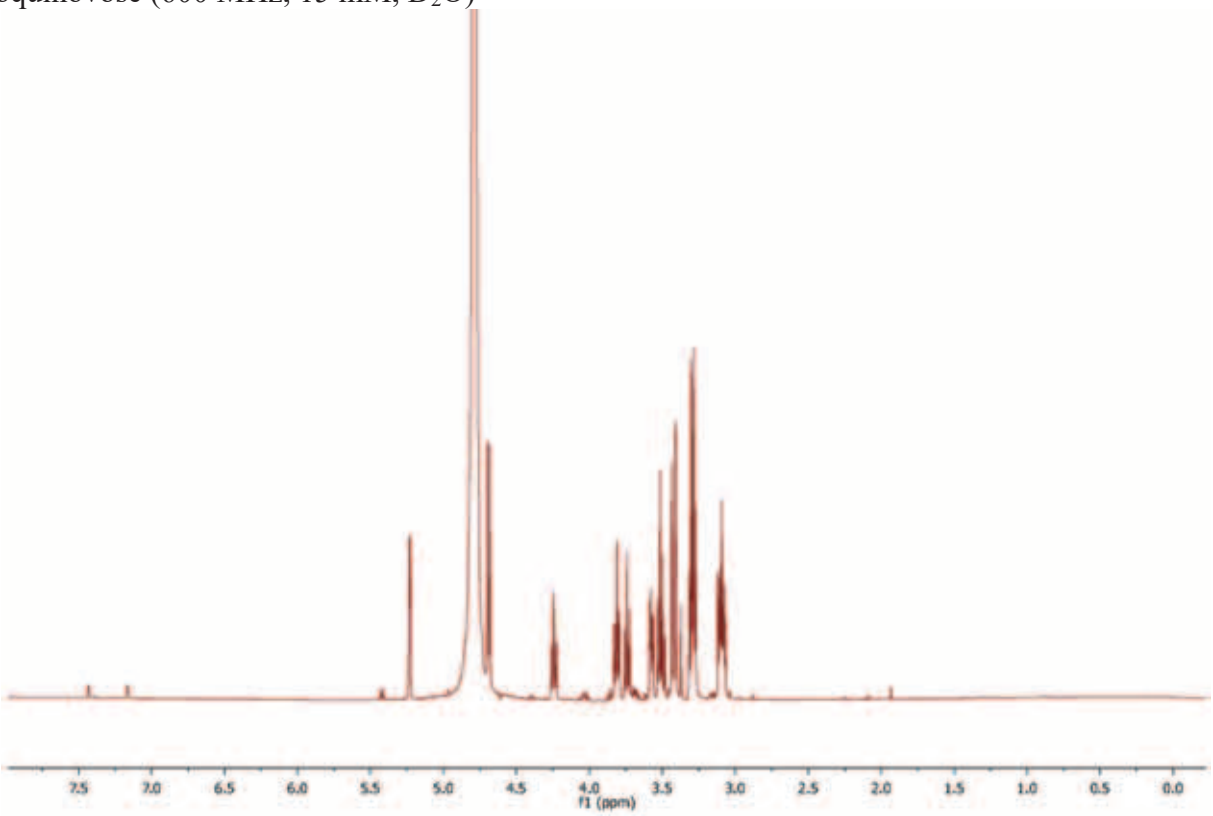

Glucose-6-phosphate (600 MHz, 15 mM, D_2O)

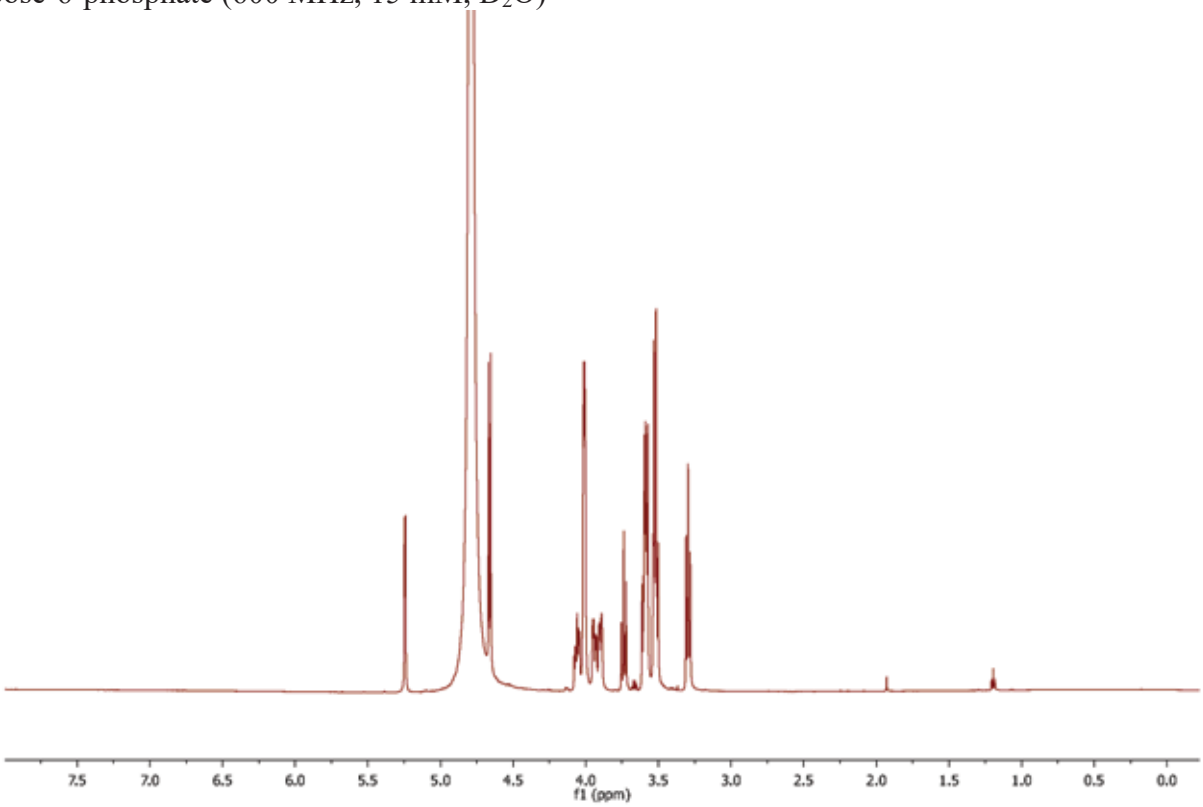

2D ^{1}H-^{1}H NOESY spectra with 1D spectrum projected onto F1 and F2 axes

Sulfoquinovose (5 mM), no enzyme

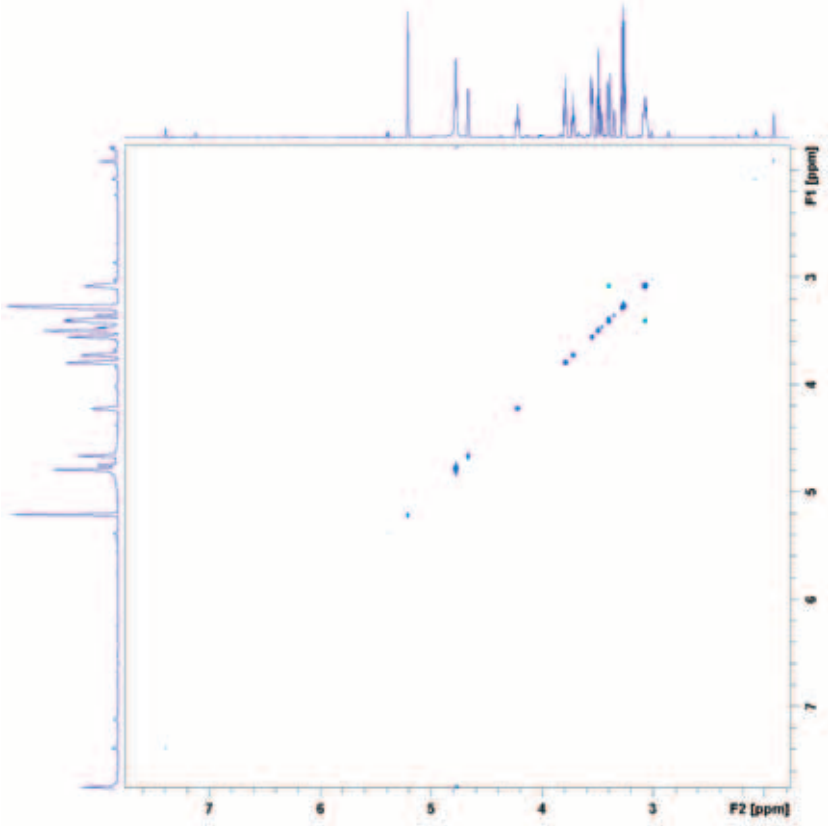

Sulfoquinovose (5 mM), with *Hs*SQM

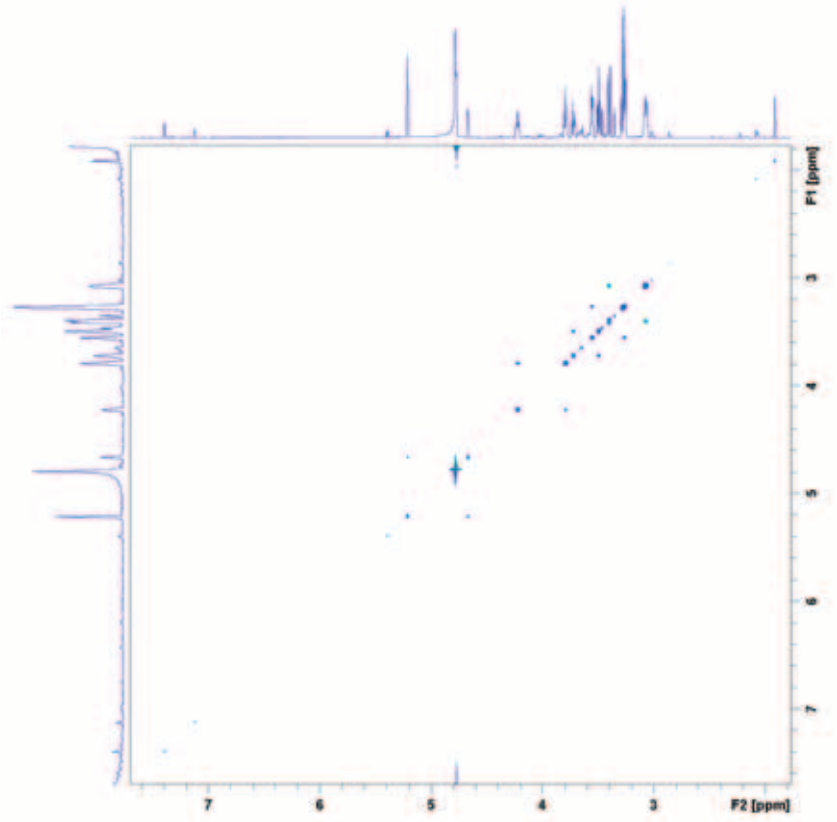

D-Glucose-6-phosphate (5 mM), no enzyme

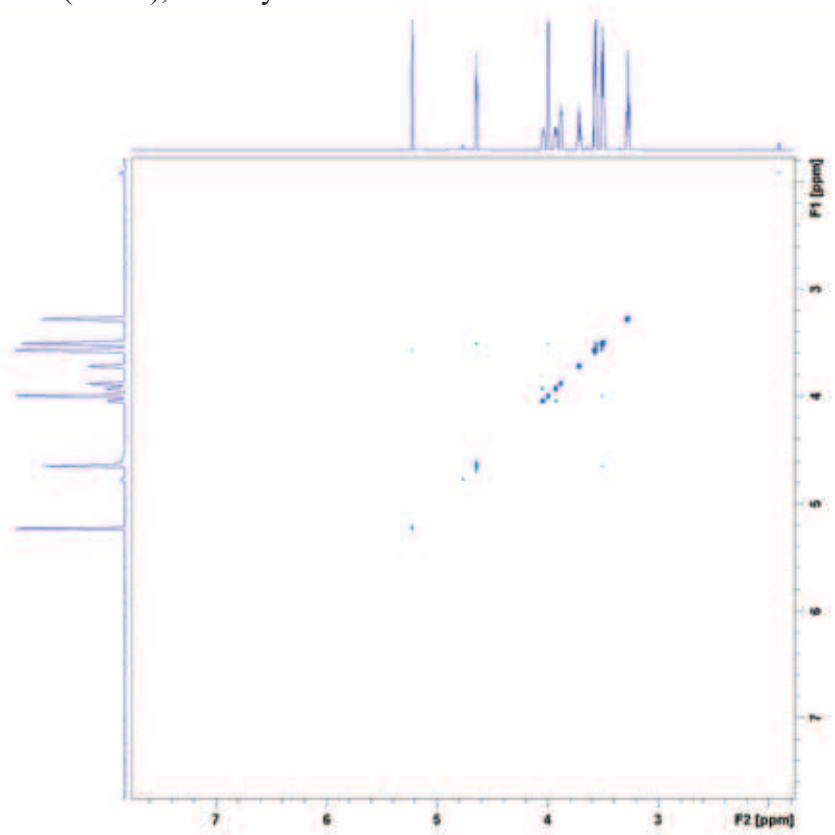

D-Glucose-6-phosphate (5 mM), with *Hs*SQM

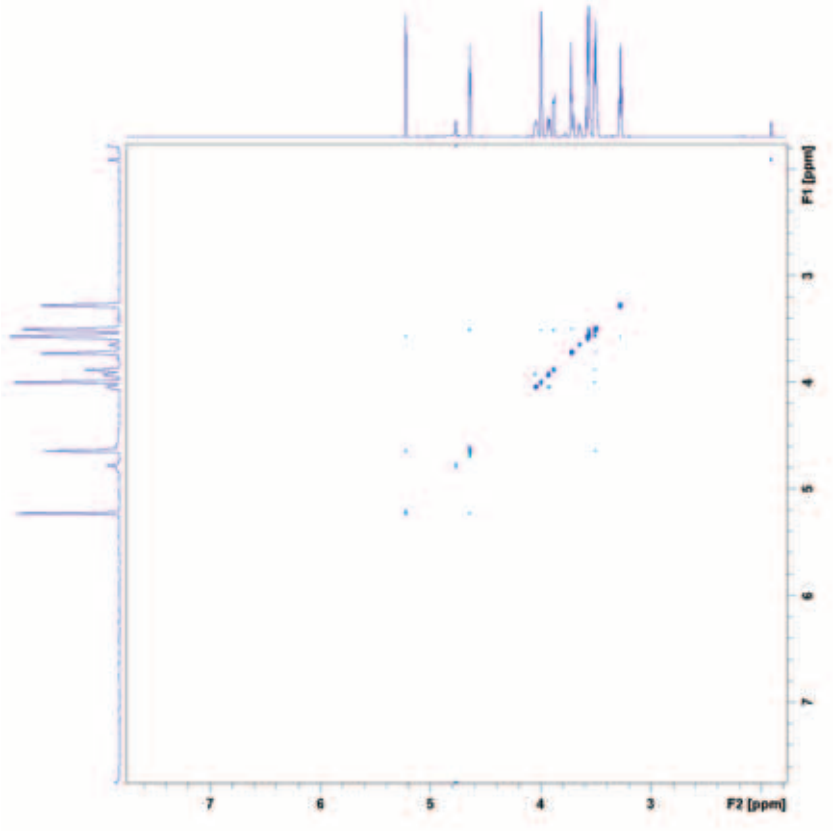

D-Glucuronic acid (5 mM), no enzyme

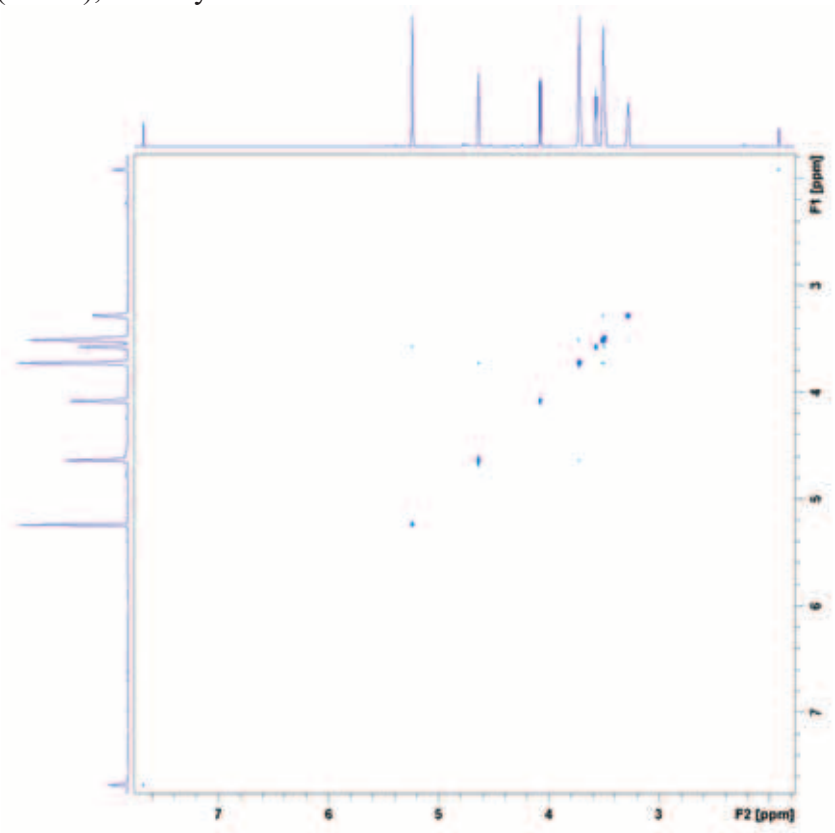

D-Glucuronic acid (5 mM), with *Hs*SQM

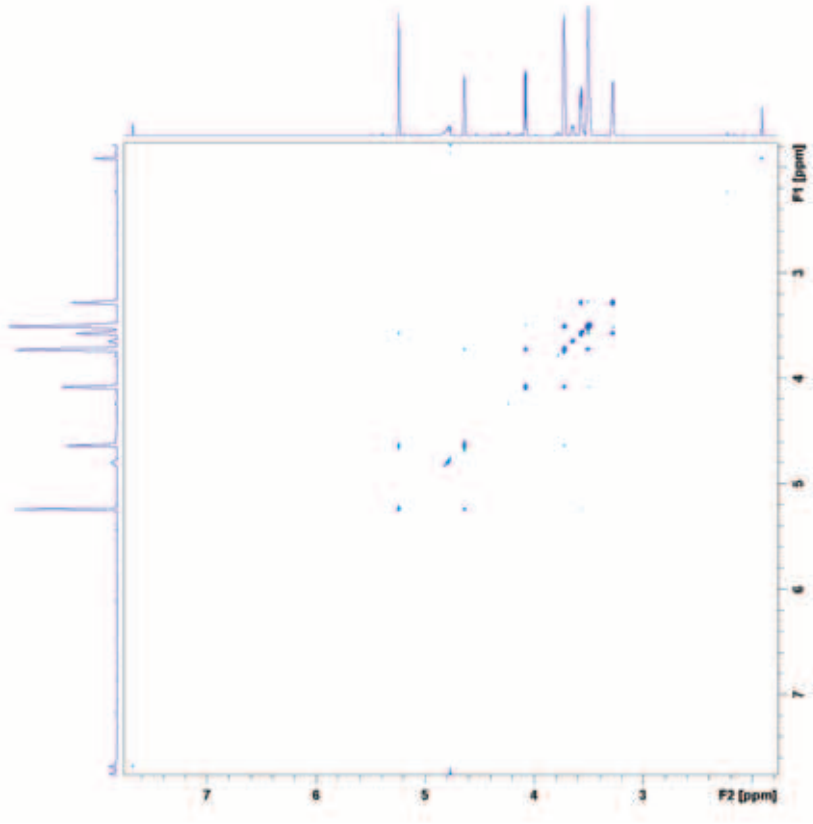

D-Glucose (5 mM), no enzyme

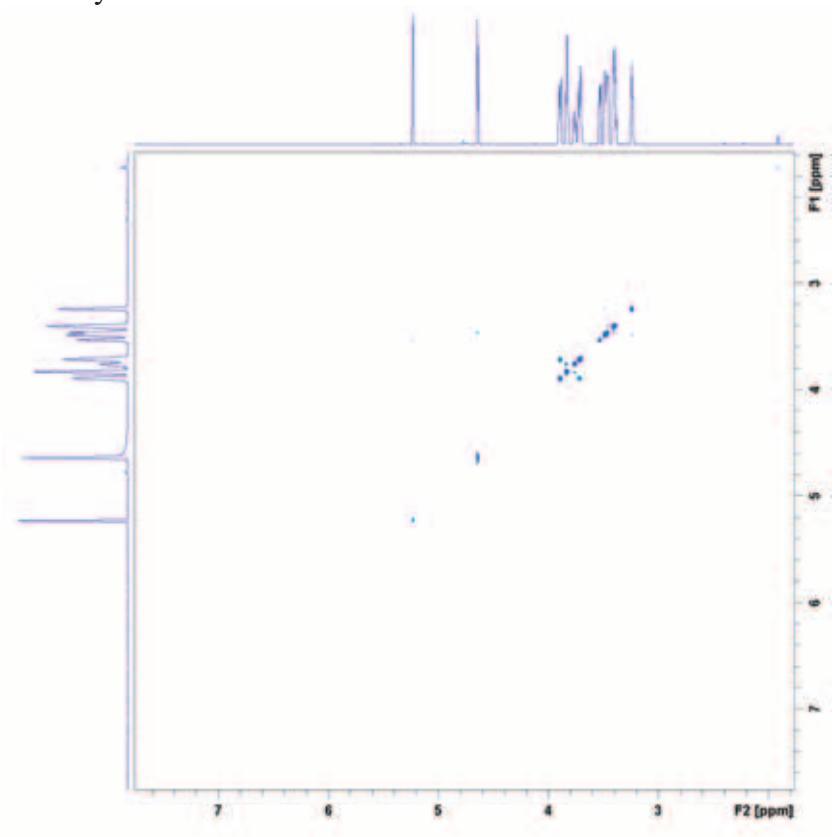

D-Glucose (5 mM), with *Hs*SQM

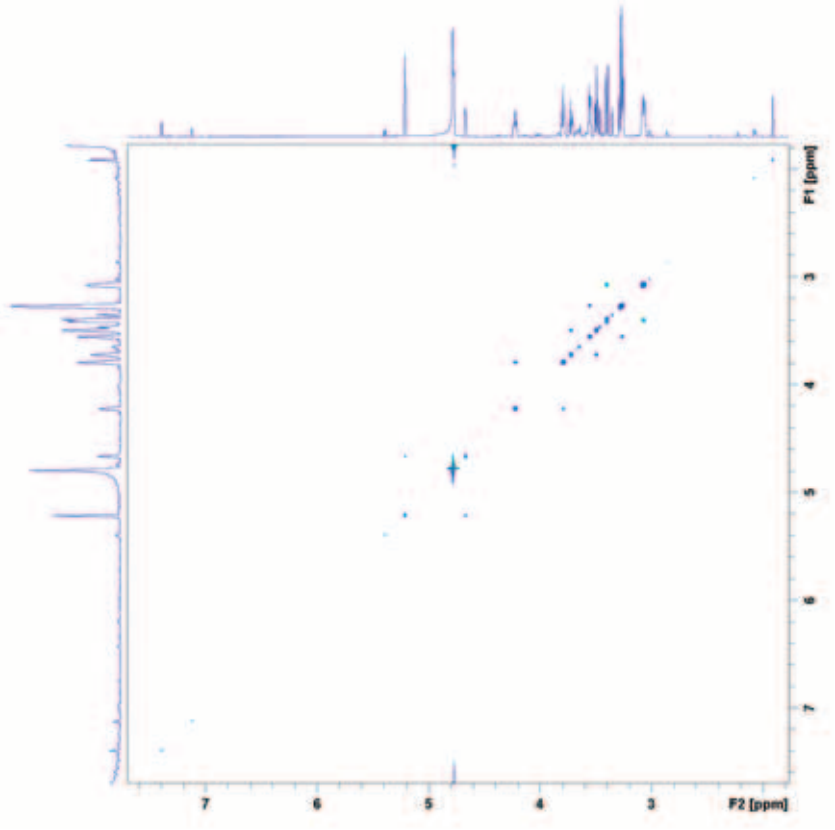

D-Galactose (5 mM), no enzyme

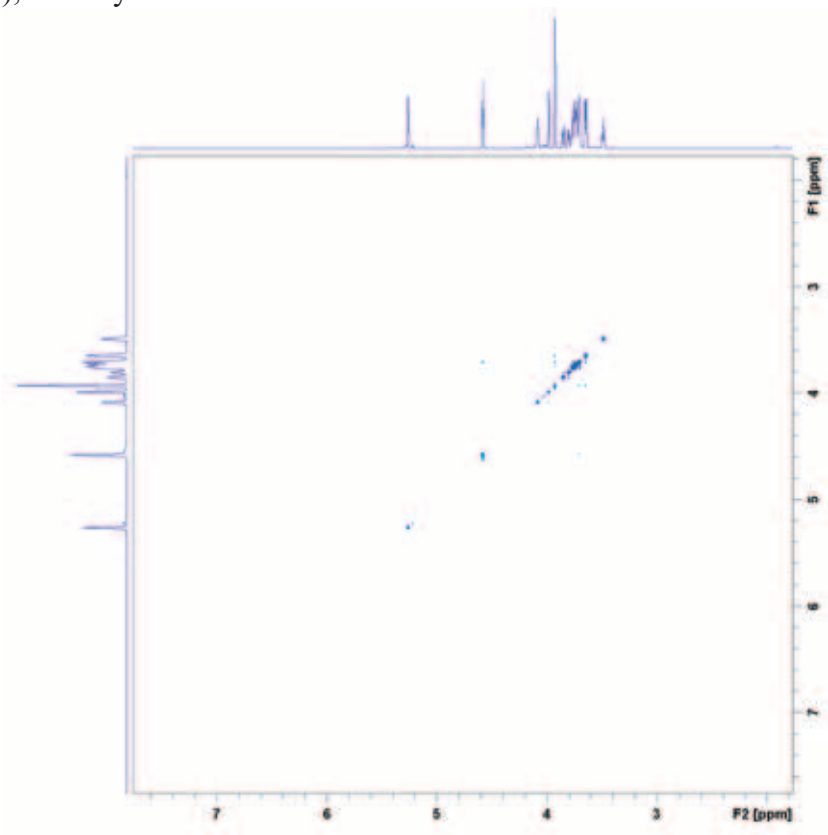

D-Galactose (5 mM), with *Hs*SQM

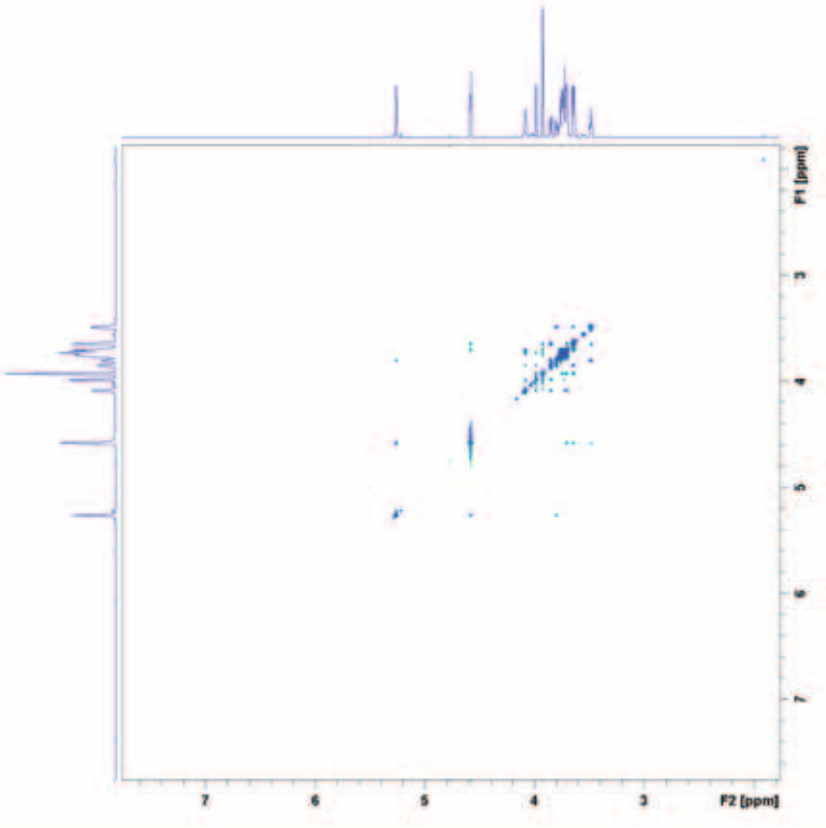

D-Mannose (5 mM), no enzyme

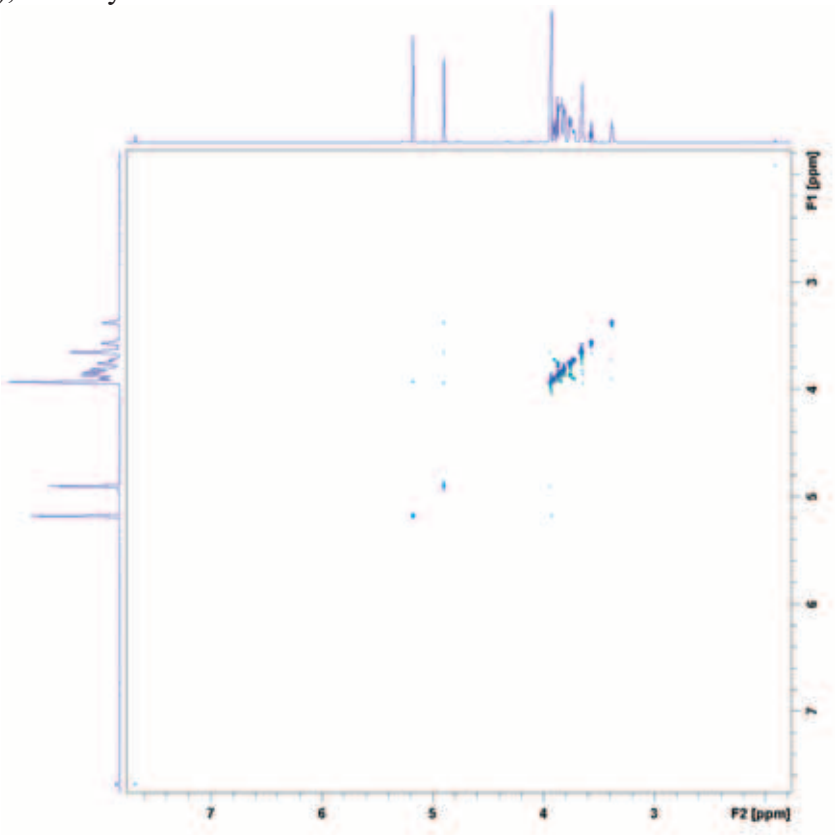

D-Mannose (5 mM), with *Hs*SQM